Long-term analysis of the sea-state in the Great Australian Bight

James, C. and Doubell, M.J.

August 2020

FRDC Project No 2018/210

© 2020 Fisheries Research and Development Corporation and South Australian Research and Development Institute.. All rights reserved.

ISBN: 978-1-876007-29-4

Long-term analysis of the sea-state in the Great Australian Bight

FRDC Project No 2018/210

2020

Ownership of Intellectual property rights
Unless otherwise noted, copyright (and any other intellectual property rights, if any) in this publication is owned by the Fisheries Research and Development Corporation and the South Australian Research and Development Institute. This work is copyright. Apart from any use as permitted under the *Copyright Act* 1968 (Cth), no part may be reproduced by any process, electronic or otherwise, without the specific written permission of the copyright owner. Neither may information be stored electronically in any form whatsoever without such permission

This publication (and any information sourced from it) should be attributed to **James, C. and Doubell, M.J. The University of Adelaide and South Australian Research and Development Institute (Aquatic Sciences), 2020, *Long-term analysis of the sea-state in the Great Australian Bight*, Final Report to the Fisheries Research and Development Corporation. Adelaide, August. CC BY 3.0]**

Creative Commons licence

All material in this publication is licensed under a Creative Commons Attribution 3.0 Australia Licence, save for content supplied by third parties, logos and the Commonwealth Coat of Arms.

Creative Commons Attribution 3.0 Australia Licence is a standard form licence agreement that allows you to copy, distribute, transmit and adapt this publication provided you attribute the work. A summary of the licence terms is available from creativecommons.org/licenses/by/3.0/au/deed.en. The full licence terms are available from creativecommons.org/licenses/by/3.0/au/legalcode. Inquiries regarding the licence and any use of this document should be sent to: frdc@frdc.com.au

Disclaimer
The authors warrant that they have taken all reasonable care in producing this report. The report has been through the SARDI internal review process, and has been formally approved for release by the Research Director, Aquatic Sciences. Although all reasonable efforts have been made to ensure quality, SARDI does not warrant that the information in this report is free from errors or omissions. SARDI and its employees do not warrant or make any representation regarding the use, or results of the use, of the information contained herein as regards to its correctness, accuracy, reliability and currency or otherwise. SARDI and its employees expressly disclaim all liability or responsibility to any person using the information or advice. Use of the information and data contained in this report is at the user's sole risk. If users rely on the information they are responsible for ensuring by independent verification its accuracy, currency or completeness.

The authors do not warrant that the information in this document is free from errors or omissions. The authors do not accept any form of liability, be it contractual, tortious, or otherwise, for the contents of this document or for any consequences arising from its use or any reliance placed upon it. The information, opinions and advice contained in this document may not relate, or be relevant, to a readers particular circumstances. Opinions expressed by the authors are the individual opinions expressed by those persons and are not necessarily those of the publisher, research provider or the FRDC.

The Fisheries Research and Development Corporation plans, invests in and manages fisheries research and development throughout Australia. It is a statutory authority within the portfolio of the federal Minister for Agriculture, Fisheries and Forestry, jointly funded by the Australian Government and the fishing industry.

Researcher Contact Details

Name:	M.J. Doubell
Address:	SARDI Aquatic Sciences, 2 Hamra Ave, West Beach 5024
Phone:	08 8429 0982
Fax:	08 8207 5481
Email:	Mark.Doubell@sa.gov.au

FRDC Contact Details

Address:	25 Geils Court
	Deakin ACT 2600
Phone:	02 6285 0400
Fax:	02 6285 0499
Email:	frdc@frdc.com.au
Web:	www.frdc.com.au

In submitting this report, the researcher has agreed to FRDC publishing this material in its edited form.

Contents

Contents ..... **iii**

Acknowledgments ..... **viii**

Abbreviations ..... **viii**

Executive Summary ..... **ix**

Introduction **1**

Objectives **2**

Method **2**

Study locations and parameters investigated 2

Data Sources and detailed parameter description 4

Fetch 6
Wind Climatology 6
Wave Climatology 6
Recent wave trends 7
Currents 8
Comparison of 2008-2012 wind and wave environment to the climatological mean 8
Wave and wind sea state thresholds 8

Results **9**

Fetch and Depth 9

Wind Climatology 11

Wave Climatology 18

Wave Trends 30

Currents 38

Comparison of 2008-2012 wind and wave environment to climatological mean 41

Wave and wind sea state thresholds 42

Discussion **46**

Implications **47**

Recommendations and Further Development **48**

Extension and Adoption **49**

Project coverage 49

Project materials developed **49**

Statistical methods and data used in this project have been adopted into model validation studies assessing the performance of ocean models developed by SARDI including the eSA-Marine (https://www.pir.sa.gov.au/research/esa_marine) South Australian Regional Ocean Model. **49**

References **49**

Tables

Table 1. The name, location and depths of sites included in this study. 3
Table 2. Model output used and periods covered. Variables include: 10m eastward (v10) and (u10) northward wind, significant wave height (Hs), peak wave period (Tp), mean wave direction (Dm), maximum wave height (Hmax), directional wave spectra (PSD), eastward (u) and northward (v) ocean current. 4
Table 3. Summary of conversions for speed units..... 5
Table 4. Fetch distances at 15 degree intervals (Direction Sectors) clockwise from due south and overall exposure estimated as the percentage of sectors not limited by fetch..... 10
Table 5. Wind speeds at return periods of 10, 25, and 100 years. Note: 1 km/h is equal to 0.54 knots 16
Table 6. Direction of maximum wind speeds with return periods of 10, 25, and 100 years..... 17
Table 7. Significant wave heights at return periods of 10, 25, and 100 years. 23
Table 8. Direction of maximum significant wave heights with return periods of 10, 25, and 100 years. 24
Table 9. Maximum wave heights at return periods of 10, 25, and 100 years. 25
Table 10. Mean wave period at return periods of 10, 25, and 100 years. 27

Figures

Figure 1. Location of model grid points for each of the four models used in the analysis (colour symbols) in relation to the requested site location shown in Table 1 (red star). Map axis are degrees longitude (x) and latitude (y). 5
Figure 2. Fetch out to 1600km at each of the four sites, green shading indicates unobstructed fetch, grey shading shows local bathymetry. 9
Figure 3. 40-year Cumulative wind direction climatology at each of the sites..... 11
Figure 4. Monthly wind climatology in the Great Australian Bight from the 40-year ECMWF-Interim model. 12
Figure 5. Monthly wind climatology for the Canadian site from the 40-year ECMWF-Interim model. 13
Figure 6. Monthly wind climatology for the Norwegian site from the 40-year ECMWF-Interim model. 14
Figure 7. Monthly wind climatology for the Brazilian site from the 40-year ECMWF-Interim model. 15

Figure 8. Wind speeds (km/hr) at return periods of 10, 25 and 100 years. Shading indicates corresponding Beaufort Scale for wind speeds. 16
Figure 9. Wind speeds (km/hr) at return periods of 10, 25 and 100 years as a function of wind direction from. 17
Figure 10. 40-year Cumulative wave direction climatology at each of the sites. 18
Figure 11. Monthly wave climatology in the Great Australian Bight from the 40-year ECMWF-Interim model. 19
Figure 12. Monthly wind climatology for the Canadian site from the 40-year ECMWF-Interim model. 20
Figure 13. Monthly wind climatology for the Norwegian site from the 40-year ECMWF-Interim model. 21
Figure 14. Monthly wind climatology for the Brazilian site from the 40-year ECMWF-Interim model. 22
Figure 15. Significant wave height at return periods of 10, 25 and 100 years. Shading indicates corresponding Douglas Sea Scale for wave heights. 23
Figure 16. Signficant wave height (m) at return periods of 10, 25 and 100 years as a function of wave direction from. 24
Figure 17. Maximum wave height at return periods of 10, 25 and 100 years. Shading indicates corresponding Douglas Sea Scale for wave heights. 26
Figure 18. Mean wave period at return periods of 10, 25 and 100 years. 27
Figure 19. Wave spectra as a function of direction and wave period. All spectra are plotted on the same intensity scale, with darker shading representing more power at that period in that sector. 28
Figure 20. Directionally integrated power spectral density (PSD) as a function of wave period at each site. The PSD is plotted in power preserving format with the area under the curve corresponding to the relative power at that frequency or period. 29
Figure 21. GAB monthly significant wave height trends from 2008 to 2018. Positive trends are indicated in red. Correlation is represented by r^2 and significance is presented as values of p where (1-p)*100% is the confidence level for a significant trend. Months for which the confidence level was less than 90% (p >0.1) are shaded out. 30
Figure 22. Canadian monthly significant wave height trends from 2008 to 2018. Positive trends are indicated in red. Correlation is represented by r^2 and significance is presented as values of p where (1-p)*100% is the confidence level for a significant trend. Months for which the confidence level was less than 90% (p >0.1) are shaded out 31
Figure 23. Norwegian monthly significant wave height trends from 2008 to 2018. Positive trends are indicated in red. Correlation is represented by r^2 and significance is presented as values of p where (1-p)*100% is the confidence level for a significant trend. Months for which the confidence level was less than 90% (p >0.1) are shaded out. 32

Figure 24. Brazilian monthly significant wave height trends from 2008 to 2018. Positive trends are indicated in red. Correlation is represented by r^2 and significance is presented as values of p where (1-p)*100% is the confidence level for a significant trend. Months for which the confidence level was less than 90% (p >0.1) are shaded out. 33
Figure 25. GAB monthly-maximum wave height trends from 2008 to 2018. Positive trends are indicated in red. Correlation is represented by r^2 and significance is presented as values of p where (1-p)*100% is the confidence level for a significant trend. Months for which the confidence level was less than 90% (p >0.1) are shaded out. 34
Figure 26. Canadian monthly-maximum wave height trends from 2008 to 2018. Positive trends are indicated in red. Correlation is represented by r^2 and significance is presented as values of p where (1-p)*100% is the confidence level for a significant trend. Months for which the confidence level was less than 90% (p >0.1) are shaded out. 35
Figure 27. Norwegian monthly-maximum wave height trends from 2008 to 2018. Positive trends are indicated in red. Correlation is represented by r^2 and significance is presented as values of p where (1-p)*100% is the confidence level for a significant trend. Months for which the confidence level was less than 90% (p >0.1) are shaded out. 36
Figure 28. Brazilian monthly-maximum wave height trends from 2008 to 2018. Positive trends are indicated in red. Correlation is represented by r^2 and significance is presented as values of p where (1-p)*100% is the confidence level for a significant trend. Months for which the confidence level was less than 90% (p >0.1) are shaded out. 37
Figure 29. Circular histograms of BRAN model current speed and direction at the four sites averaged over 11 years and 0-50 m depth. 38
Figure 30. Circular histograms of BRAN model current speed and direction at the four sites averaged over 11 years and 50-200m depth. 39
Figure 31. Circular histograms of BRAN model current speed and direction at the four sites averaged over 11 years and 200-4000 m depth. 40
Figure 32. Comparison of average wave and wind conditions for 2008-2012 period with the long term (1979-2018) climatological averages and standard deviations. 41
Figure 33. Full 40-year Hs model output for all four sites, highlighting, by colour, periods of 5 or more days below the specified significant wavehight threshold. The percentage of time as a function of the entire record where these conditions were met are summarized next to each time series. 42
Figure 34. Estimated number of days a year with 5 consecutive days of significant wave height below the threshold limit. 43
Figure 35. Full 40-year wind speed output for all four sites, highlighting, by colour, periods of 5 of more days below the specified wind speed thresholds. The percentage of time as a function of the entire record where these conditions were met are summarized next to each time series. .. 44

Figure 36. Estimated number of days a year with 5 consecutive days of wind speed below the threshold limits. 45

Acknowledgments

Thank you to Kirsten Rough from the Australian Southern Bluefin Tuna Industry Association (ASBTIA) for her helpful discussions which contributed to the development and improvement of this report. We also thank the reviewers and editor for their comments which improved the quality of the report. This study was funded through the Fisheries Research and Development Corporation (FRDC) ASBTIA Industry Partnership Agreement (IPA).

Abbreviations

ASBTIA - Australian Southern Bluefin Tuna Industry Association
FRDC - Fisheries Research and Development Corporation
GAB - Great Australian Bight
IMOS - Integrated Marine Observing System
met-ocean - meteorological and oceanographic
SARDI – South Australian Research and Development Institute
PIRSA – Primary Industries and Regions South Australia

Executive Summary

The Australian Southern Bluefin Tuna Industry Association operates in shelf and offshore waters of the Great Australian Bight (GAB). In recognition of the exposed nature of this environment, there has been concern from commercial fisheries and the community regarding its suitability for hosting offshore petroleum activities. This report presents information on the meteorological and oceanographic (met-ocean) conditions which contribute to the sea-state experienced at a deep water petroleum permit location in the GAB. Comparisons with three other major international offshore petroleum locations are made to place the GAB findings in a global context. Since long time-series of direct observations for the relevant met-ocean parameters are not available for the GAB location, data from several global data-assimilating and re-analysis atmospheric and oceanographic models are used to determine the monthly climatological conditions and the probability of extreme events for each location. Comparison of the four locations show that the two North Atlantic sites, Canada and Norway, are exposed to stronger winds and larger waves than the GAB site, while Brazil has the lowest winds and smallest waves by a large margin. Winds at the GAB site are characterized by a pronounced seasonal signal, and are on average stronger in summer and winter than during the spring and autumn. Predominant wind directions at the GAB site are from the southeast in summer and southwest in winter, with wind speeds less than 15 knots for 5 consecutive days occurring on average 55 days per year. The GAB site is also exposed to a remarkably consistent swell, with significant wave heights persistently exceeding 2.5 m from the southwest and an average wave period of 16s. While other sites do experience calm wave conditions from time to time, the GAB site is rarely calm, with significant wave heights less than 2.5 m over 5 consecutive days occurring only 35 days per year on average. Compared to other sites, the GAB showed the largest change in current directions with depth, with currents below 200 m directed onshore/alongshore and to the northeast-east.

This report provides for a clearer understanding of the met-ocean conditions encountered offshore in the GAB. The characterisation and comparison of wind, wave and current climatology's and extreme events in the GAB relative to other major international petroleum sites provides quantitative information necessary for fishing and aquaculture sectors, and the broader community, to assess the long-term environmental risks of offshore petroleum activities in the region.

Keywords

Great Australian Bight, sea-state, oceanography, meteorology, waves, wind, currents, return periods, extreme events, ocean models

Introduction

The Great Australian Bight (GAB) forms part of the world's longest southern continental shelf boundary, and its temperate marine ecosystems support a wide range of natural resources of economic and ecological importance (Rogers et al. 2013, 2015, Goldsworthy et al. 2017, Ward et al. 2006). Regional productivity is underpinned by extensive seasonal upwelling (Kämpf *et al.* 2004, van Ruth *et al.* 2019), which provides food and habitat for a range of iconic and endangered species, apex predators and multiple high-value commercial fisheries (e.g. Southern Bluefin Tuna, *Thunnus maccoyii*; Australian Sardine, *Sardinops sagax*; Southern Rock Lobster, *Jasus edwardsii;* Greenlip and Blacklip Abalone, *Haliotis rubra rubra and Haliotis laevigata*, and Western King Prawn, *Melicertus latisulcatus*). The uniqueness, productivity and ecology of the GAB positions it as a place of global conservation significance (Rogers et al. 2015).

Studies of the inter- and intra- seasonal variation in meteorological forcing experienced in the GAB have provided insight into their influence on ocean circulation (Middleton and Bye 2007), coastal dynamics (i.e. upwelling/downwelling) (Kämpf *et al.* 2004, Doubell *et al.* 2019), and ecosystem productivity (van Ruth *et al.* 2019). Recent studies (Doubell *et al.* 2019, van Ruth *et al.* 2019) have benefited from *in situ* oceanographic measurements made available through the Integrated Marine Observing System, which has been operating in the eastern GAB region since 2008. In addition, research outcomes from the Great Australian Bight Research Program have increased our understanding of the regional oceanography across the broader GAB region (Middleton *et al.* 2017). Despite this, a detailed climatological assessment of the meteorological and oceanographic conditions which contribute to the sea state experienced in deeper waters, offshore from the continental shelf, in the central GAB region has been constrained by limited direct observations, due to the remoteness of the location and the difficulties and expense associated with the deployment and recovery of observing equipment.

The Australian Southern Bluefin Tuna Association (ASBTIA) operates in shelf and offshore waters of the GAB. In recognition of the exposed and remote nature of the offshore GAB environment, ASBTIA have requested information to better understand the climatology of the meteorological and oceanographic (met-ocean) conditions which contribute to the 'sea state' experienced at a deep water petroleum permit location in the GAB. The study uses long-time series of relevant parameters obtained from global, data-assimilating, ocean models to provide a quantitative description and prediction of the conditions likely to be experienced in the GAB. Comparisons are made with other major international offshore deep water petroleum locations

identified by ASBTIA to provide a greater understanding of the environmental conditions in the GAB in a global context. The purpose of this report is to present a clear description and prediction of the prevailing and extreme environmental conditions encountered offshore in the GAB. An understanding of these conditions is critical to assessing petroleum industry development, and incident response plans relevant to the long-term sustainability of South Australian fishing and aquaculture sectors, as well as the social acceptance of the petroleum industry with stakeholder's and the broader community.

Objectives

The main objective of this report is to provide a greater understanding of the meteorological and oceanographic conditions experienced in the GAB at a deep-water petroleum permit location. Specific objectives include:

1. To understand the exposure and sea-state of the GAB relative to three other major international offshore deep water petroleum locations.
2. For each location, provide a summary of the monthly sea-state climatology described by the mean, variance, frequency and intensity.
3. For each location, determine the probability of extreme events occurring at specified return periods.

Method

Study locations and parameters investigated

In addition to the Stromlo-1 Ceduna Sub Basin site in the GAB, three additional major international offshore deep water petroleum sites were identified and selected by ASBTIA for comparison with the GAB site (Table 1). The international sites include Bay du Nord (Canada), Espirito Basin (Brazil), and the Norwegian Sea (Norway). The location of each site is summarized in Table 1.

Table 1. The name, location and depths of sites included in this study.

Site	Country	Latitude	Longitude	Depth (m)
Ceduna Sub Basin	Australia	34.9000^{O}S	130.7667^{O}E	2240
Bay du Nord	Canada	48.86331^{O}N	47.0651^{O}W	800-1200
Espirito Basin	Brazil	20.0817^{O}S	40.0686^{O}W	1800
Norwegian Sea	Norway	65.1125^{O}N	6.8901^{O}E	300-500

For each site, we undertook an analysis of the meteorological and oceanographic parameters described below, to better understand the environmental conditions relevant to petroleum activities. In summary, these parameters include:

1. **Fetch**: The depth and distance to land around 15 degree segments of the compass. Including a map of the bathymetry.
2. **Wind Climatology**: The monthly averaged wind speed, direction and frequency to determine the probability of extreme winds events for pre-determined segments around the compass and for return periods 10, 25 and 100 years.
3. **Wave Climatology**: The monthly average significant wave height, mean wave period, maximum wave height and mean wave direction to determine the probability of extreme wave events for pre-determined segments around the compass and for return periods 10, 25 and 100 years.
4. **Recent Wave Trends**: Trends in the significant and maximum wave height for each month over the period January 2008 to present.
5. **Currents**: Current speed and direction at each site over several depth intervals (e.g. 0-50 m, 50-200 m and greater than 200 m).

In addition, this report will address the following additional questions requested by ASBTIA:

a. For comparison with previous statistical reports presented on the met-ocean conditions in the GAB, how did wind and wave environment over the 2008-2012 period compare to the long-term climatological mean?
b. At each site, how frequent were occurrences of 5 or more consecutive days of significant wave height (Hs) below thresholds of 4.5, 3.5, 2.5 and 1.5 m?
c. At each site, how frequent were occurrences of 5 or more consecutive days of wind speeds below thresholds of 10, 15, 20 and 30 knots.

Data Sources and detailed parameter description

Model output from four distinct, data assimilating global models was compiled to address the project objectives. A description of the models and parameters used, their spatial resolution and the periods for which model output is available, is provided in Table 2. Table 3 provides conversions for wind speeds in knots, km/h, m/s and Beaufort scale.

For 10m surface wind components to the east (u10) and north(v10), significant wave height (i.e. defined as the average of the largest 1/3 of the waves) (Hs), peak wave period (Tp) and mean wave direction (Dm) the ECMWF ERA-Interim atmospheric model (Dee *et al.* 2011) was used. For maximum wave height (i.e. the largest wave observed) (Hmax), the ECMWF CERA-20C model (Laloyaux *et al.* 2018) was used. For directional wave spectra (PSD), the CSIRO CAWCR Wave hindcast and reanalysis model (Durrant *et al.* 2014) was used. For the ocean currents (u, components to the east (u) and north(v), output from the CSIRO's Bluelink Reanalysis (BRAN) model version 3p5 (Oke *et al.* 2012) was used.

Since each model output is given on distinct discrete spatial grids, there is typically some discrepancy between the requested location of the site to be analysed and the data point from the model grid. In the case of the four (model) data sources we have reasonable agreement in the locations (Fig. 1), with the lower resolution CAWCR grid usually providing the least accurate location. In addition to the met-ocean model data, the ETOPO1 global topography from NOAA (Amante and Eakins 2009) was used to provide depth information on a $1/30^{O}$ resolution grid.

Table 2. Model output used and periods covered. Variables include: 10m eastward (v10) and (u10) northward wind, significant wave height (Hs), peak wave period (Tp), mean wave direction (Dm), maximum wave height (Hmax), directional wave spectra (PSD), eastward (u) and northward (v) ocean current.

Model	**Source**	**Variables**	**Period Covered**	**Spatial Resolution**
ERA-Interim	ECMWF	Hs,Tm,Dm,u10,v10	Jan 1979 – Jul 2018	0.75^{O}
CERA-20C	ECMWF	Hmax	Jan 1970 – Jan 2010	1.0^{O}
CAWCR	CSIRO	PSD	Jan 2008 – Dec 2018	Variable: $0.4\text{-}5.0^{O}$
BRAN 2015	CSIRO	u, v	April 2009 - Jan 2019	0.1^{O}

Table 3. Summary of conversions for speed units.

knots	km/h	m/s	Beaufort
1	1.85	0.51	0
1-3	1-5	0.51-1.54	1
4-6	6-11	2.06-3.09	2
7-10	12-19	3.60-5.14	3
11-15	20-28	5.66-7.72	4
16-21	29-38	8.23-10.80	5
22-27	39-49	11.31-13.89	6

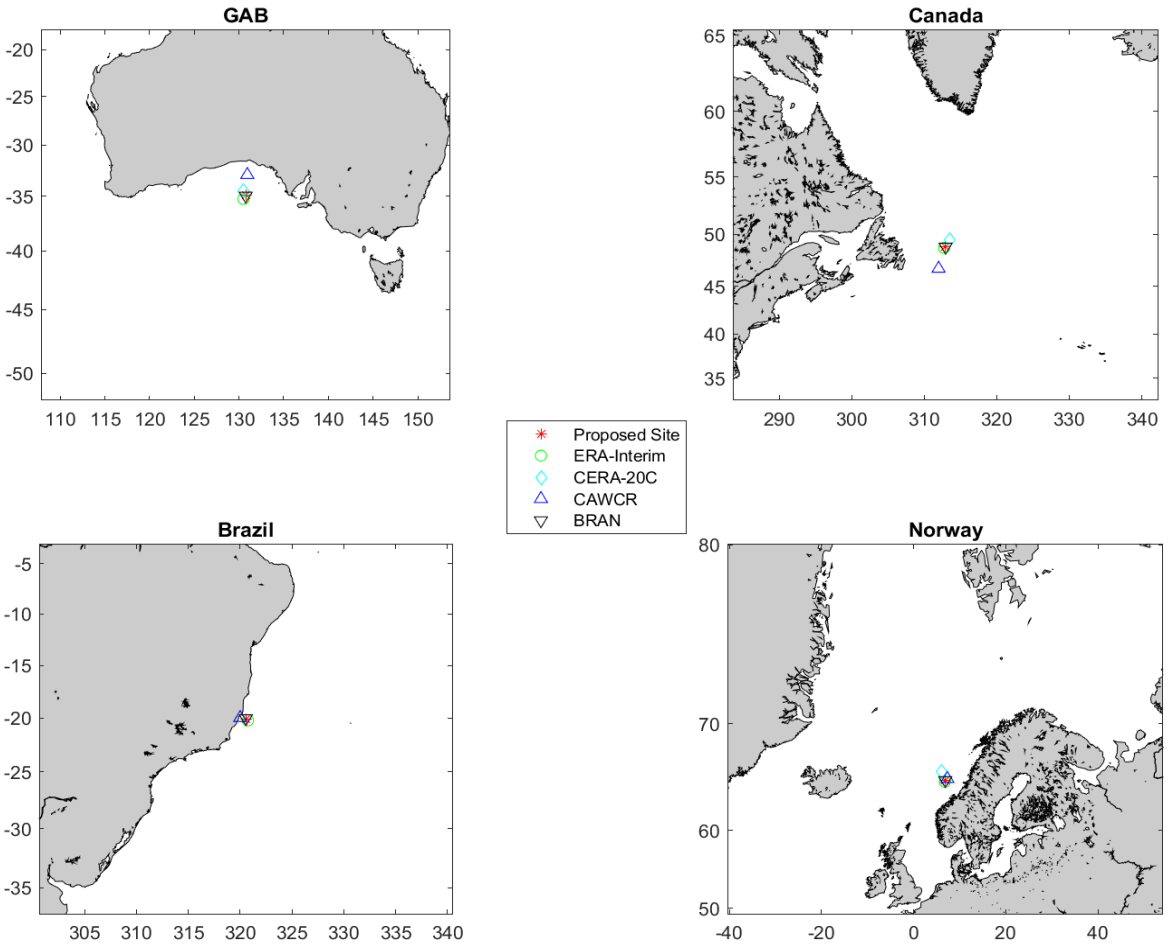

Figure 1. Location of model grid points for each of the four models used in the analysis (colour symbols) in relation to the requested site location shown in Table 1 (red star). Map axis are degrees longitude (x) and latitude (y).

Below is a description of the methods used to provide information on the meteorological and oceanographic conditions which contribute to the sea state for each location investigated in this study.

Fetch

Fetch is technically the distance to the nearest land point in the direction from which the wind is blowing. In practice, for a given location we determine fetch as the distance to land around the compass in 15^{O} intervals. In relation to open ocean waves, fetch is one of several factors which influences wave size and the energy contained within waves. Other factors include the speed and duration of the wind and the area over which it is experienced.

The ETOPO1 global topography (Amante and Eakins 2009) was used for bathymetry and to determine the presence of land. The topography was filtered twice using a second order Shapiro filter to eliminate very small islands which are expected to have no significant impact on fetch. Fetch was then determined by the distance to the nearest land mass within that sector with an upper limit of 1600 km. This upper limit is generous as wave heights are expected to become independent of fetch after approximately 500 km (Darbyshire 1952).

Wind Climatology

Estimates of 10m wind speeds (u10, v10) were obtained from the ERA-Interim product over a period of approximately 39 years (Table 2). The monthly climatology was then calculated for speed and direction around 30^{O} intervals at each site. Wind speed return values were calculated using the Gringorten method (Gringorten 1963) and were based on modelling the tail of a Gumbel distribution applied to the probability distribution of yearly maximum values. Wind speed return periods were calculated for 10, 25 and 100 years as a function of direction.

Wave Climatology

Estimates of significant wave height (Hs), mean wave period (Tm), and mean wave direction (Dm) were obtained from the ERA-Interim product (Table 2). Significant wave height (Hs) represents the average of the highest one third of waves in the wave spectrum and is considered to be the best estimate of the wave field (Sverdrup and Munk 1947). Estimates of the mean wave period (Dp) and mean wave direction (Dm) describe the period and direction

of the waves averaged over the entire spectrum. Maximum wave height (Hmax) is the height of the largest wave occurring in the wave spectrum and is much harder to estimate. The maximum wave height occurs infrequently, with estimates based on a Rayleigh distribution of 1 in 3000 waves having a height equal to twice the Hs (Dean 1990), with some observational evidence that the maximum wave height may exceed significant wave height by up to a factor of three (Stansell 2005).

We note that wave heights are ultimately limited by the steepness of a wave, which is a function of the wave's height and length, where wave steepness is estimated as $kH/2$ where $k = 2\pi/L$ is the wavenumber, and H and L are the wave height and wavelength, respectively. Detailed studies (Toffoli *et al.* 2010) on the shape of waves have shown well defined threshold values for the wave steepness above which waves can no longer sustain their shape and break. The threshold value for the front-face steepness is equivalent to a steepness of 0.55 and for rear-face steepness the threshold value is approximately 0.44.

Because maximum wave height is not provided in the standard ERA-Interim product, predictions of Hmax were taken from the CERA-20C product. Monthly climatology of Hs and Dm were calculated around 30^{O} intervals at each site. Return values for Hs, Tm, and Hmax were calculated using the Gringorten method (Gringorten 1963) and based on modelling the tail of a Gumbel distribution applied to the probability distribution of yearly maximum values. Return periods were calculated for 10, 25 and 100 years. A return period analysis was also applied to the Hs values as a function of direction using the Dm values.

Recent wave trends

To estimate recent trends in sea state, ECMWF ERA-Interim values of Hs were binned into monthly averages from January 2008 to December 2018. The maximum wave heights (Hmax) from the ECMWF CERA-20a model runs do not cover this period, so the monthly maximum wave heights at each site were estimated using the directionally integrated CAWCR wave spectra and analysed for trends over the Jan 2008-Dec 2018 period (Table 2). Linear regression was used to determine the sign of the slope, positive for increasing trend. The statistical significance of the trend was determined as a confidence level from the degrees of freedom (N), the correlation coefficient (r), and the student-t test (Bendat and Piersol, 1986).

Currents

Currents from the last 10 years (April 2009 to January 2019) were extracted from the BRAN 2015 global ocean model for the four sites (Table 2). Vertical and temporal averages of currents over the last decade and at three depth ranges were plotted as a function of direction. The depth ranges selected were 0 to 50 m, 50 to 200 m, and 200 to 4000 m or the maximum depth at each location.

Comparison of 2008-2012 wind and wave environment to the climatological mean

Winds and significant wave height (Hs) were extracted from the ECMWF ERA-Interim model output (Table 2) and the average values for each month over the period 2008-2012 were compared with the long-term 40-year monthly climatology.

Wave and wind sea state thresholds

ECMWF ERA-Interim significant wave heights (Hs) and wind speed values were used to determine the number of consecutive days that the sea state was below each of four threshold values. Threshold values for Hs were 4.5, 3.5, 2.5 and 1.5 m. Threshold values for wind speed were 10, 15, 20 and 30 knots. Periods longer than 5 days were highlighted. Estimates of the number of days each year where the sea state remained below each of the thresholds from the 40-year time series were calculated.

Results

Fetch and Depth

Plots of directional fetch at each of the sites (Figure 2) indicate that fetch is not a limiting factor at any site, as all sites have an unobstructed distance of greater than 1600 km in multiple sectors. Fetch distances are broken down into 15^{O} sectors and shown in Table 3, with a summary of exposure estimated as the overall percentage of sectors not limited by fetch. The Canadian site has the greatest exposure (i.e. wider window), while the Norwegian site has the least.

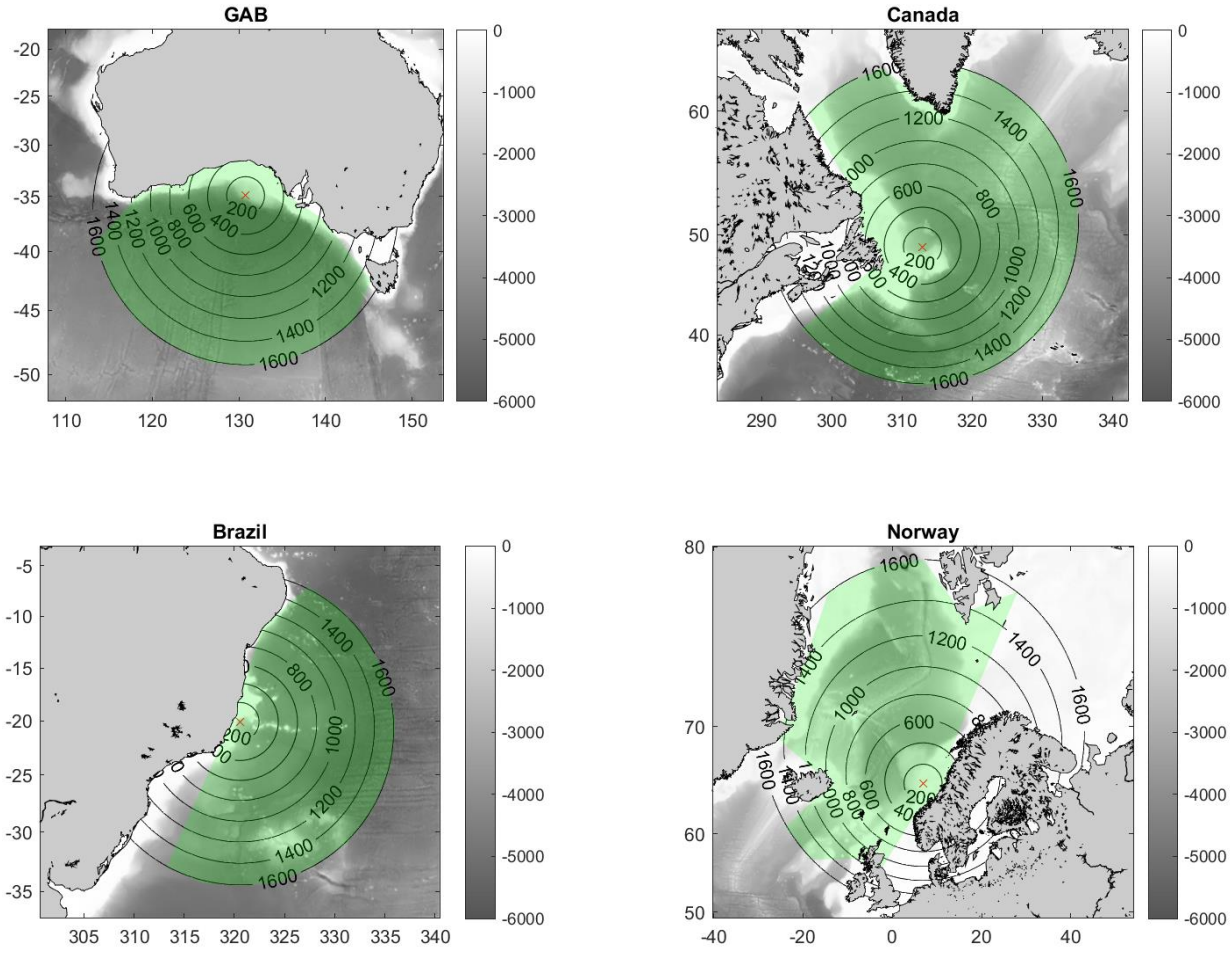

Figure 2. Fetch out to 1600km at each of the four sites, green shading indicates unobstructed fetch, grey shading shows local bathymetry.

Table 4. Fetch distances at 15 degree intervals (Direction Sectors) clockwise from due south and overall exposure estimated as the percentage of sectors not limited by fetch.

Direction Sectors (degrees T)	GAB (km)	Canada (km)	Brazil (km)	Norway (km)
-180	1600	1600	1600	245
-165	1600	1600	1600	315
-150	1600	1600	1600	1171
-135	1600	1600	275	1175
-120	1600	1600	160	1600
-105	1600	440	104	1600
-90	1140	484	103	972
-75	663	694	78	1458
-60	523	756	80	1401
-45	431	1600	83	1450
-30	418	1600	85	1600
-15	399	1600	176	1600
0	371	1336	266	1600
15	368	1600	1016	1363
30	388	1600	1600	1600
45	402	1600	1600	413
60	384	1600	1600	376
75	423	1600	1600	286
90	441	1600	1600	229
105	853	1600	1600	205
120	1517	1600	1600	214
135	1600	1600	1600	225
150	1600	1600	1600	200
165	1600	1600	1600	242
Exposure	38%	79%	54%	25%

Wind Climatology

Wind direction and speeds for each of the sites based on the 40-year ECMWF model data are shown in Figure 3. Sites show varying degrees of directionality and strength. For example, in Brazil winds are generally relatively weak (<= 40 km/h) and blow consistently out of the northeast. In the GAB, the strongest winds (60 km/h) blow out of the southwest and wind speeds exceeding 40 km/h frequently occur out of all points of the compass. At the two North Atlantic sites the influence of the persistent and strong westerlies (~ 70 km/h) can be seen, with the most common direction varying between west and southwest at the Canadian and Norwegian sites.

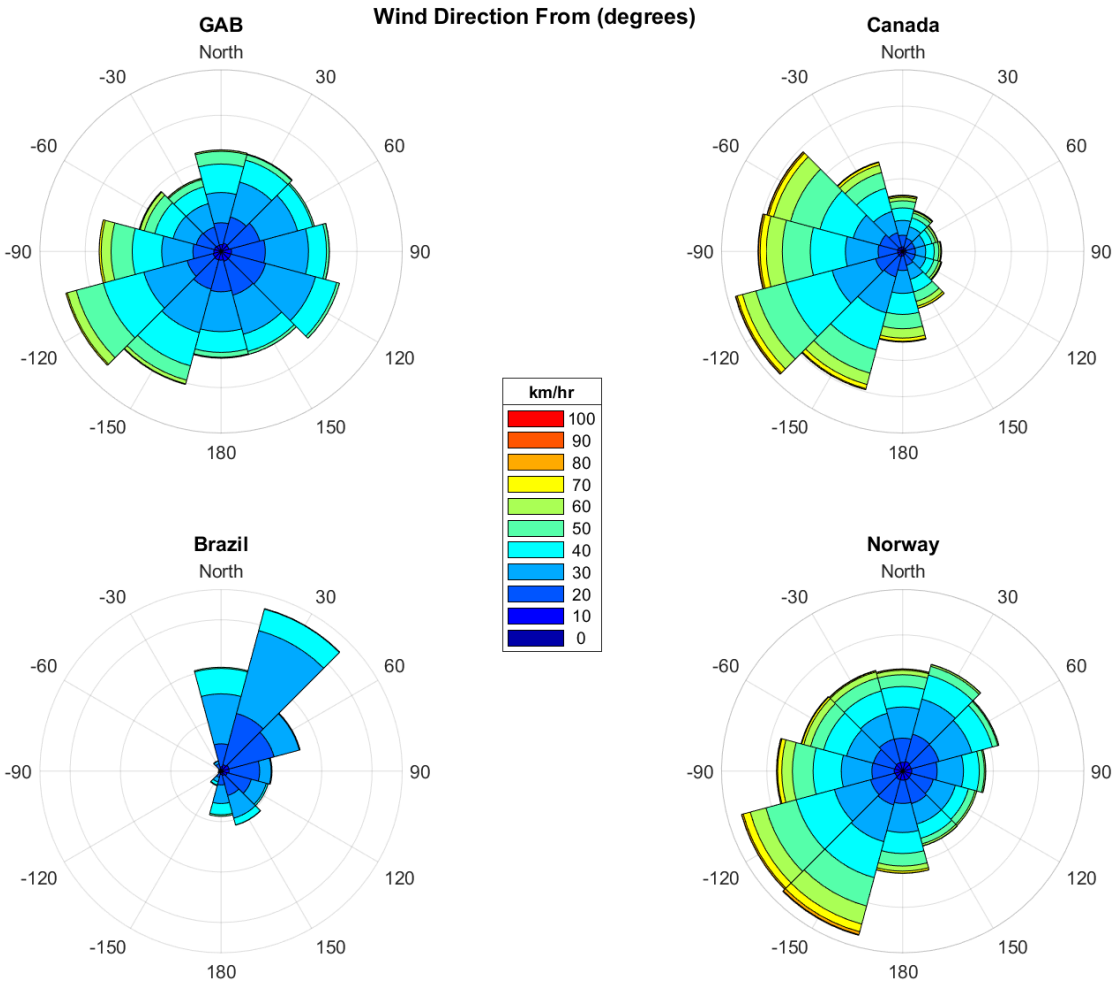

Figure 3. 40-year Cumulative wind direction climatology at each of the sites.

A breakdown of site by month indicates the seasonal nature of wind direction at each of the sites (Figures 4-6). In general, the strongest winds are found from directions not limited by fetch (Figure 2).

The seasonal nature of the winds in the GAB are shown in Figure 4 and are well documented (Middleton and Bye 2007). In summary, weather in the GAB is dominated by alternating low and high pressure systems moving from west to east, hence winds are experienced over a wide range of directions, with southerly/south-westerly changes associated with the passing of low pressure systems. Summer coastal upwelling is driven by winds from the southeast while winter conditions are dominated by stronger winds from the southwest.

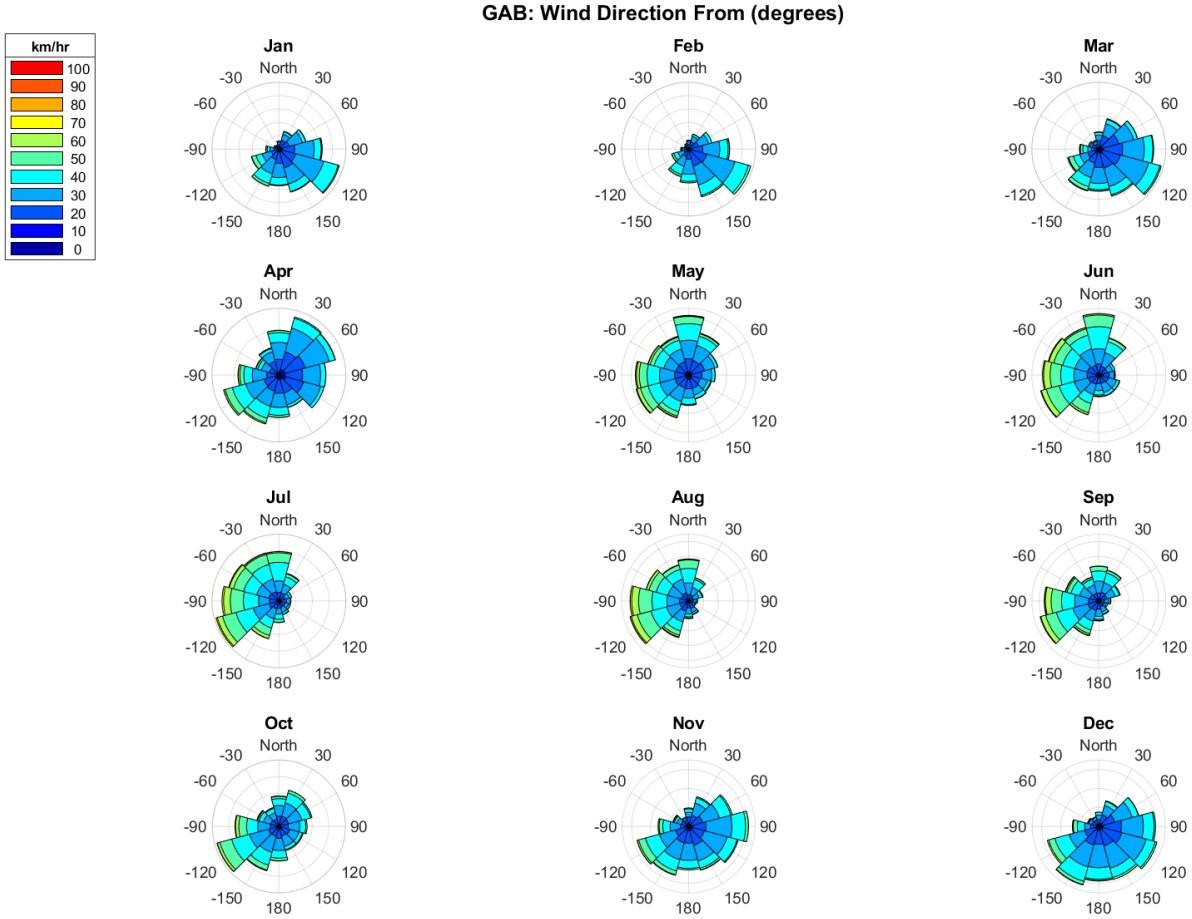

Figure 4. Monthly wind climatology in the Great Australian Bight from the 40-year ECMWF-Interim model.

The seasonal winds at the Canadian site (Figure 5) are dominated by strong westerlies during the winter months and milder south-westerlies during the summer months.

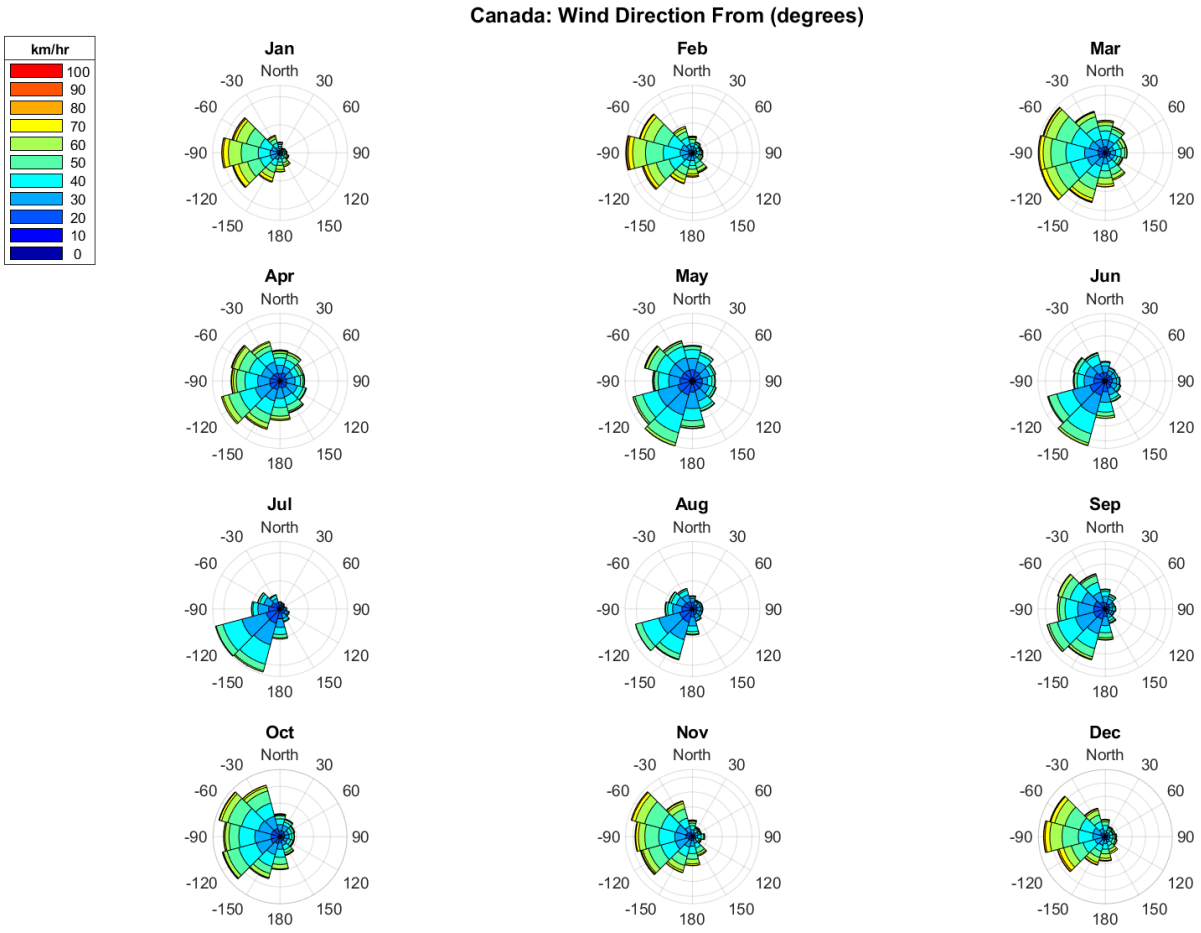

Figure 5. Monthly wind climatology for the Canadian site from the 40-year ECMWF-Interim model.

Similarly to the Canadian Site, the Norwegian site (Figure 6) is dominated by very strong winter winds and relatively mild summer winds. The winds are predominantly from the southwest during the winter and from southwest and northeast during the summer.

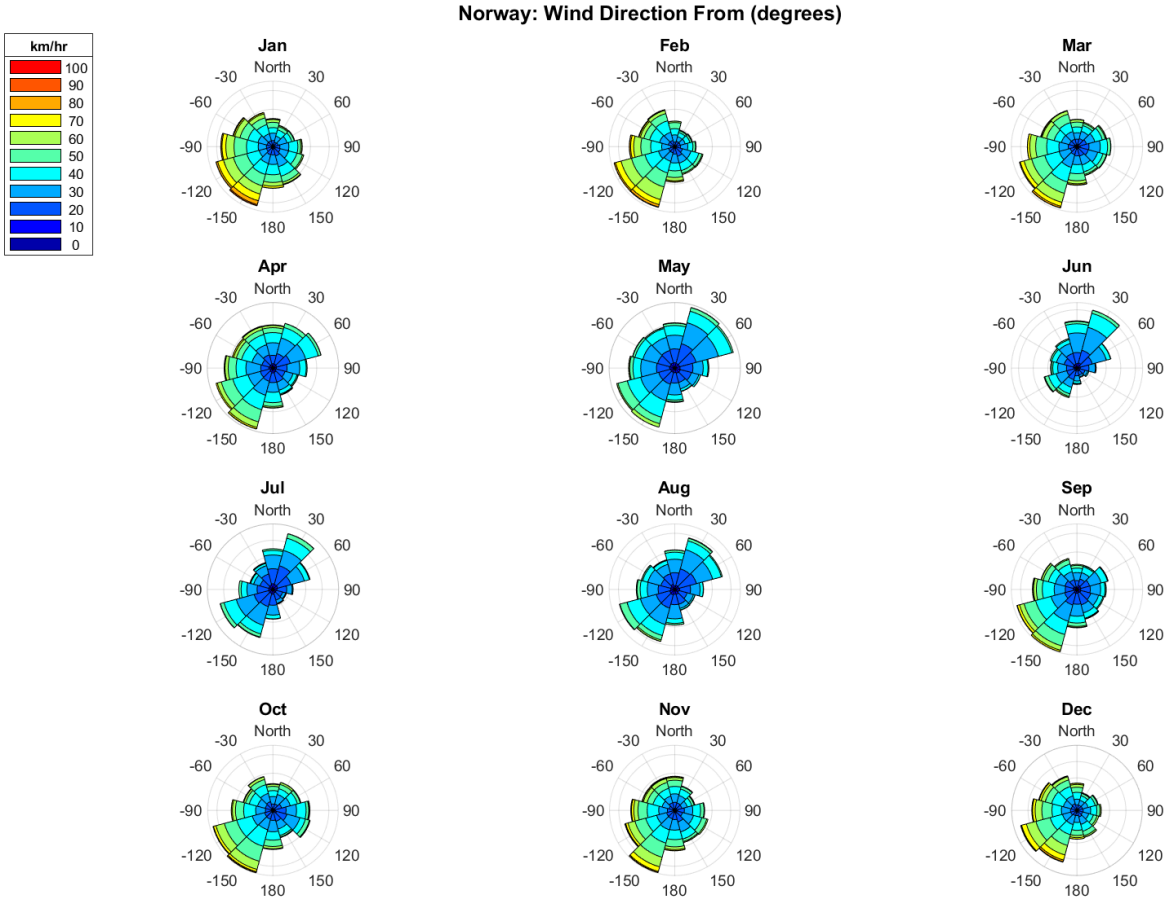

Figure 6. Monthly wind climatology for the Norwegian site from the 40-year ECMWF-Interim model.

The winds at the Brazilian site (Figure 7) are much milder than those at the other sites. From late winter to early spring (August to March) the winds are consistently from the northeast switching to more variable during the spring and early summer Months (April to July).

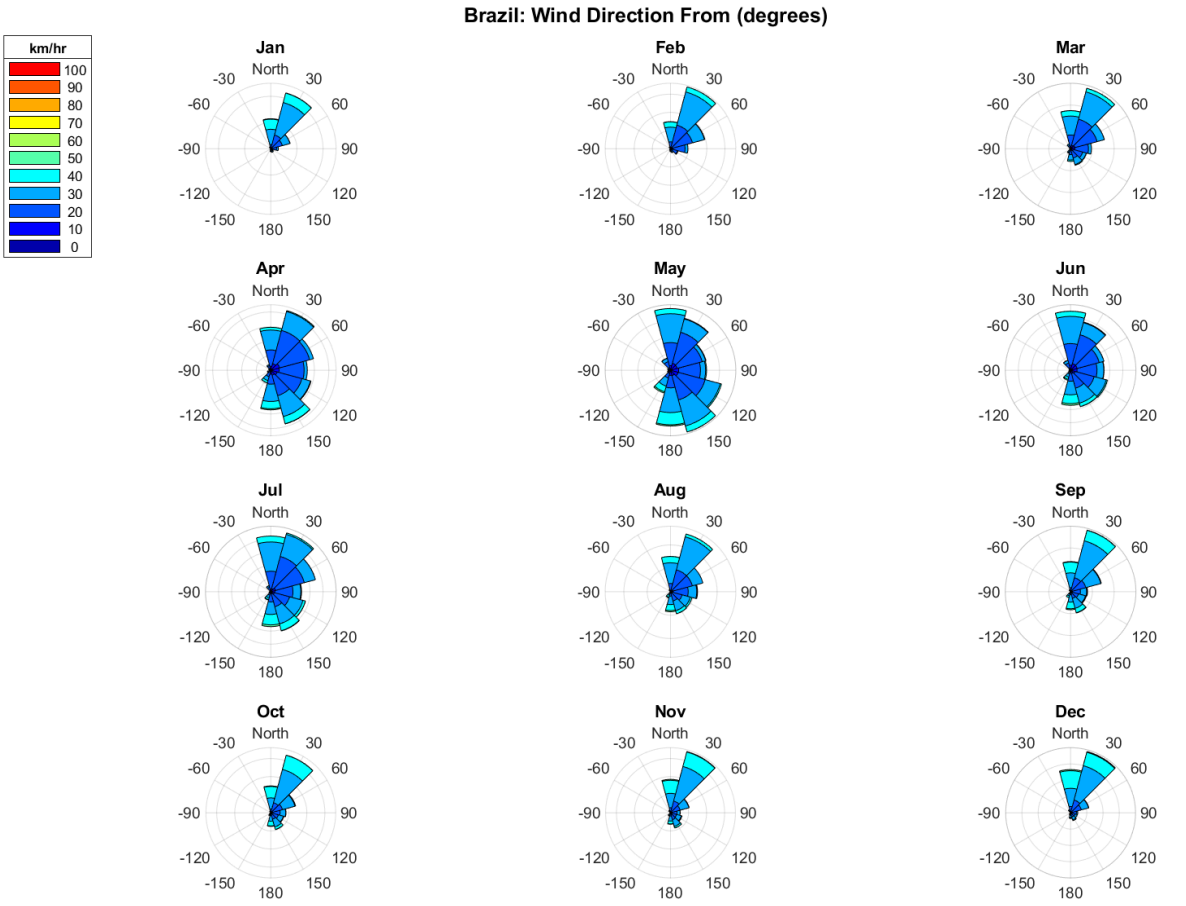

Figure 7. Monthly wind climatology for the Brazilian site from the 40-year ECMWF-Interim model.

Analysis of the return periods for wind speeds at each location is shown in Figure 8, with return periods for 10, 25 and 100 years at each location summarized in Table 4. All sites except Brazil would expect to experience full Gale force winds (force 8-10, >62 km/hr) on a regular basis (<1 year return period), but only the Canadian site would expect force 11 winds (1 category below Hurricane) and then only with a return period of 100 years. The Brazilian site 100-year wind event is less than the 25-year wind event predicted at the three other sites and less than an annual event at the Canadian and Norwegian sites. Note that the extreme wind event (~100 km/hr) in the GAB approaches a 1000-year wind event under the Gumbel distribution even though it was captured within a 40-year observation window.

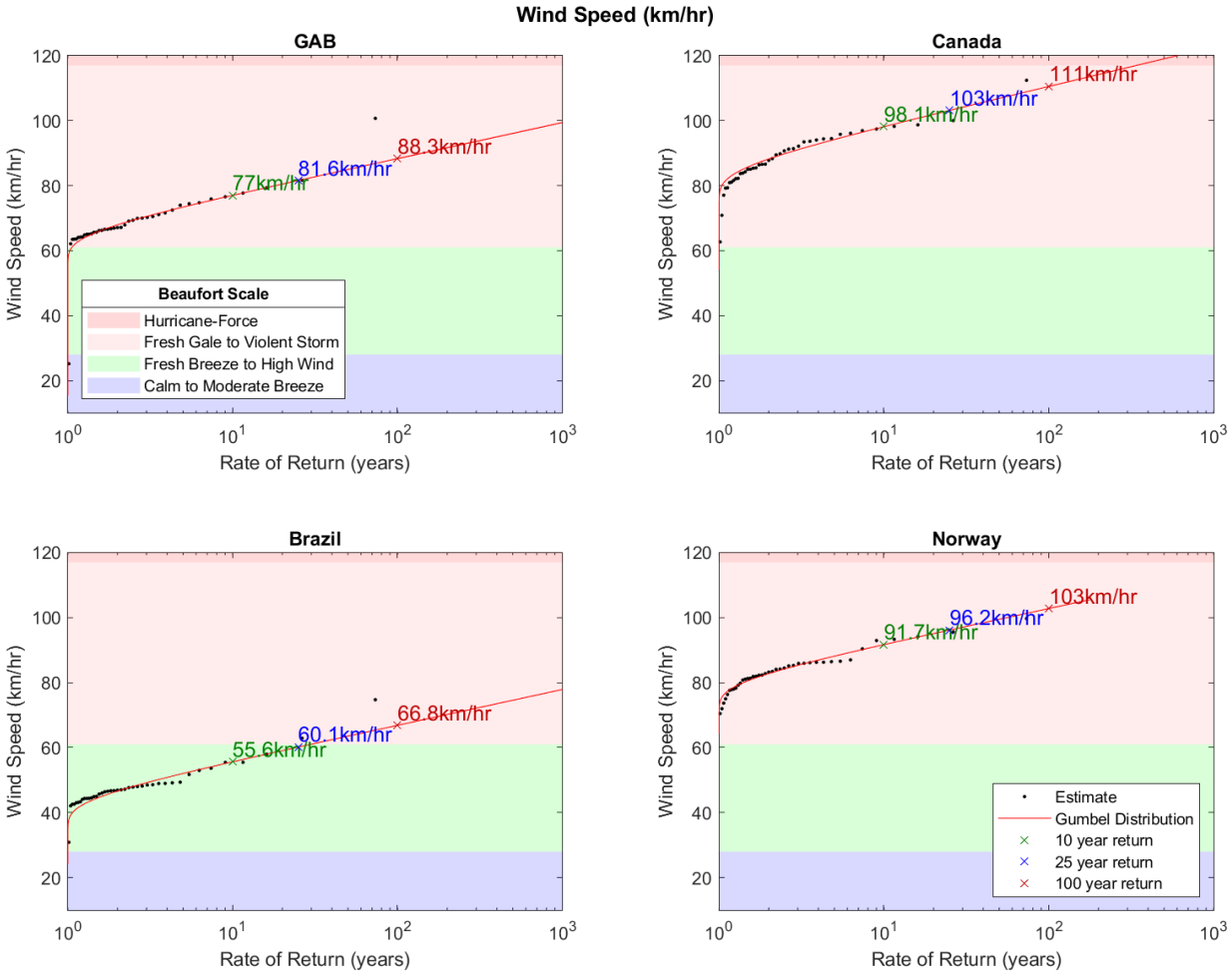

Figure 8. Wind speeds (km/hr) at return periods of 10, 25 and 100 years. Shading indicates corresponding Beaufort Scale for wind speeds.

Table 5. Wind speeds at return periods of 10, 25, and 100 years. Note: 1 km/h is equal to 0.54 knots

Return Period (years)	GAB (km/hr)	Canada (km/hr)	Brazil (km/hr)	Norway (km/hr)
10	77.0	98.1	55.6	91.7
25	81.6	103.1	60.2	96.2
100	88.3	110.5	66.9	102.8

The return period wind speeds as a function of direction are shown in Figure 9. Again, the direction of maximum winds tends to be from directions of non-limited fetch (see Figure 2). The specific values for the direction of maximum winds are presented in Table 5. Note that these values differ slightly from the directionally independent wind speeds given in Table 4 since the probability distributions used in the analysis differ when calculated as a function of direction.

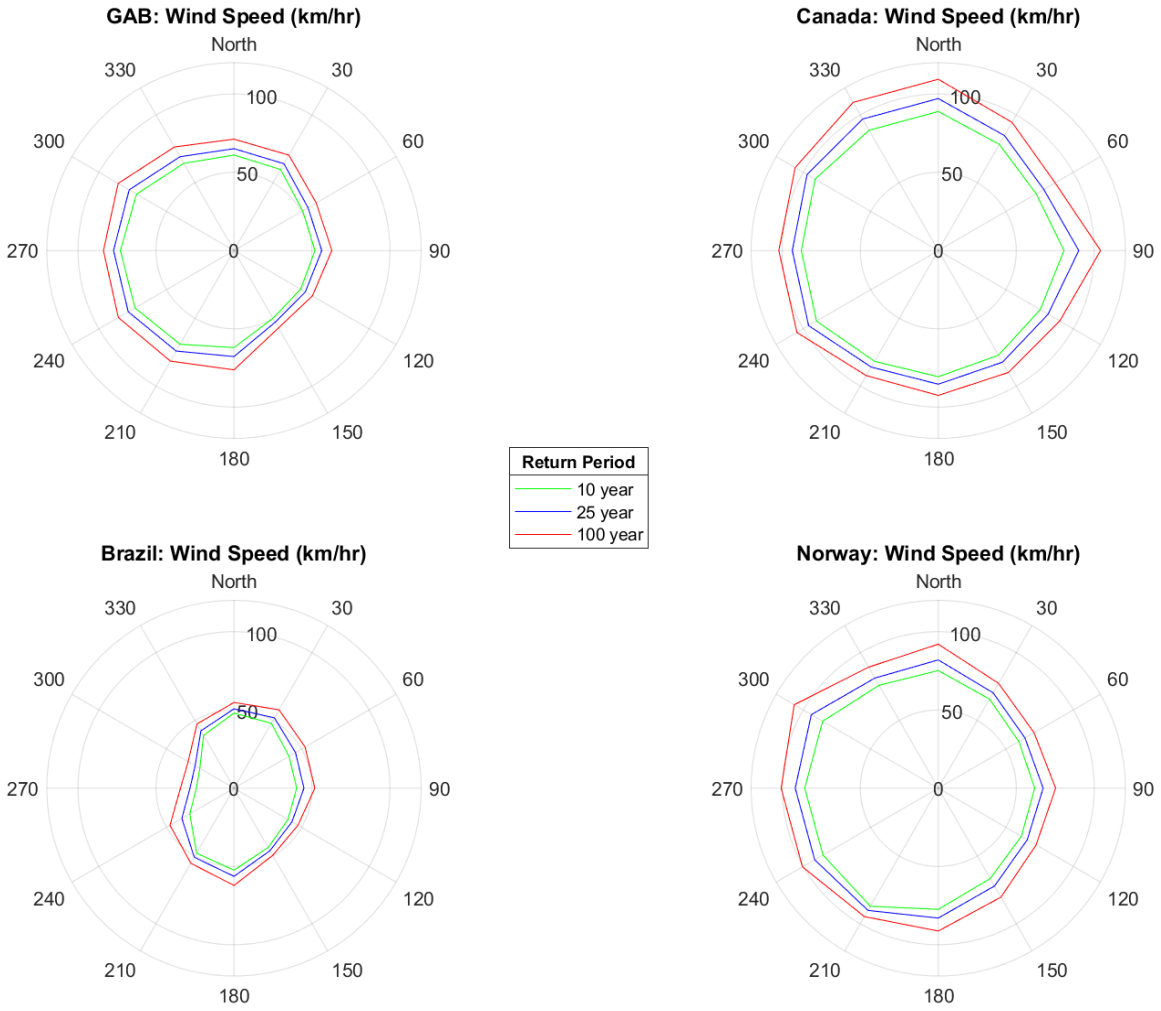

Figure 9. Wind speeds (km/hr) at return periods of 10, 25 and 100 years as a function of wind direction from.

Table 6. Direction of maximum wind speeds with return periods of 10, 25, and 100 years.

	10 year		**25 year**		**100 year**	
	Direction	Speed	Direction	Speed	Direction	Speed
GAB	-120	73.3	-120	78.3	-60	85.7
Canada	-60	91.2	-60	97.1	0	109.4
Brazil	180	52.3	180	56.3	180	62.1
Norway	-150	87.1	-60	93.9	-60	106.6

Wave Climatology

For each site, the wave climatology (Figure 10) shows stronger directionality (i.e. less variability) than the wind climatology (Figure 3). Large swell waves are formed by weather systems which are typically not local, while smaller wind waves are generated by local winds. Large waves (>6 m) are found at all sites except Brazil, this is consistent with Brazil also having the weakest wind climatology. Waves in the GAB are consistently greater than 3 m and are from the southwest with maximum sizes comparable to those in Canada and Norway.

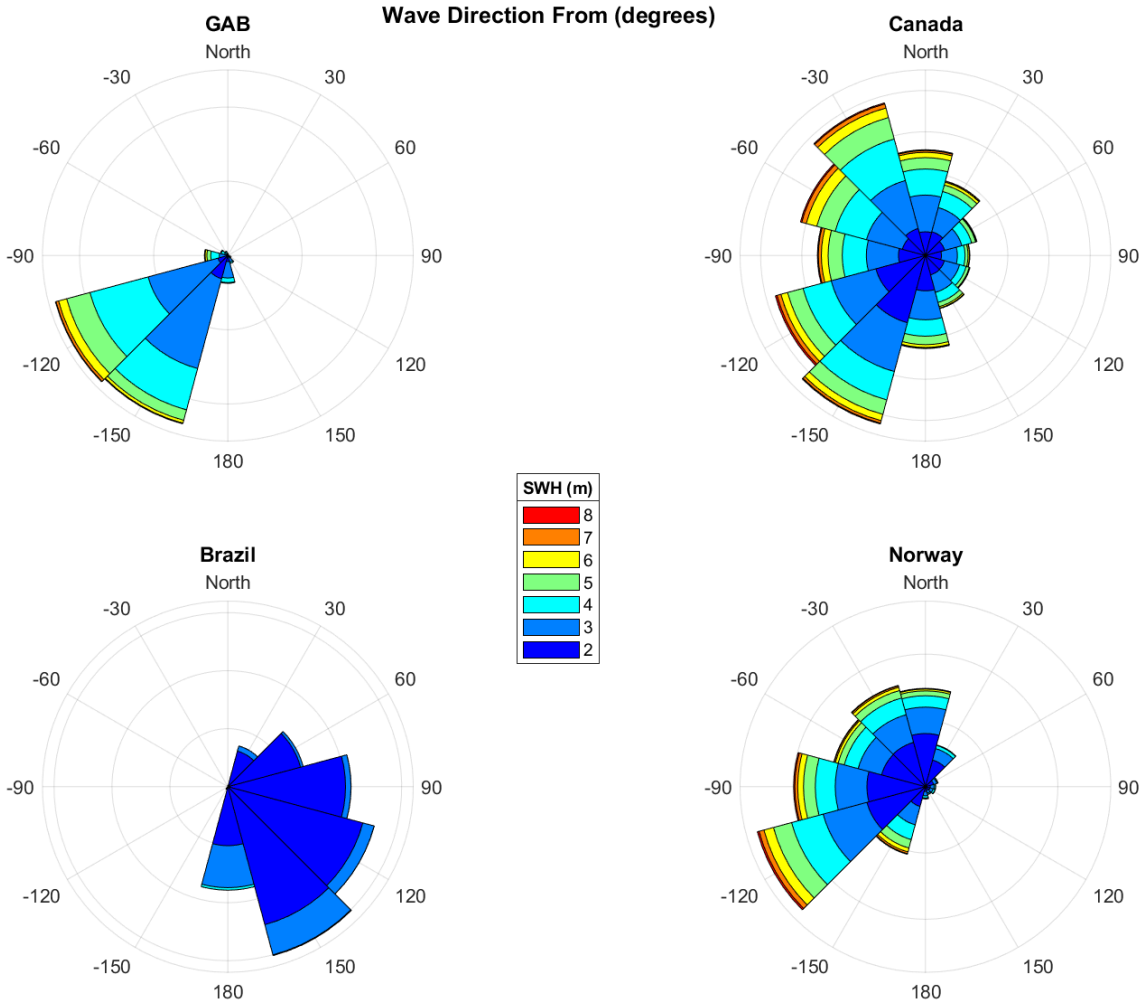

Figure 10. 40-year Cumulative wave direction climatology at each of the sites.

Figure 11 shows the wave climatology at the GAB site by month. The GAB has the least variable directional wave climatology of all the sites, with significant waves only coming from the south-west year round despite having fairly open exposure to the Southern Ocean. The consistency of direction across all months in the GAB is unique when compared to the other locations. There is also little evidence of waves with significant wave height (Hs) less than 3 m at any time. Consistent with the GAB monthly wind climatology (Figure 4), waves are stronger from the west, south-west, during the southern hemisphere winter, before moderating and shifting to be from the south, south-west during the summer. During all months the direction of the wave field is persistently on-shore.

Figure 11. Monthly wave climatology in the Great Australian Bight from the 40-year ECMWF-Interim model.

At the Canadian site the largest waves appear to be along a wide range of directions with most coming from the Labrador Sea to the northwest and from the southwest out of the North Atlantic (Figure 12). The monthly breakdown of the Canadian wave climatology shows a strong seasonal pattern. During the northern hemisphere winter very large waves (>7 m) tend to originate out of the Labrador Sea to the west and northwest. During the spring, the waves

transition to a much milder summer wave climate with significant wave heights generally less than 3 m and coming out of the southwest. During the autumn, the waves begin to build again before returning to the large winter wave configuration. Another significant point is that the prevailing wave direction tends to be into the North Atlantic rather than towards the Canadian coast.

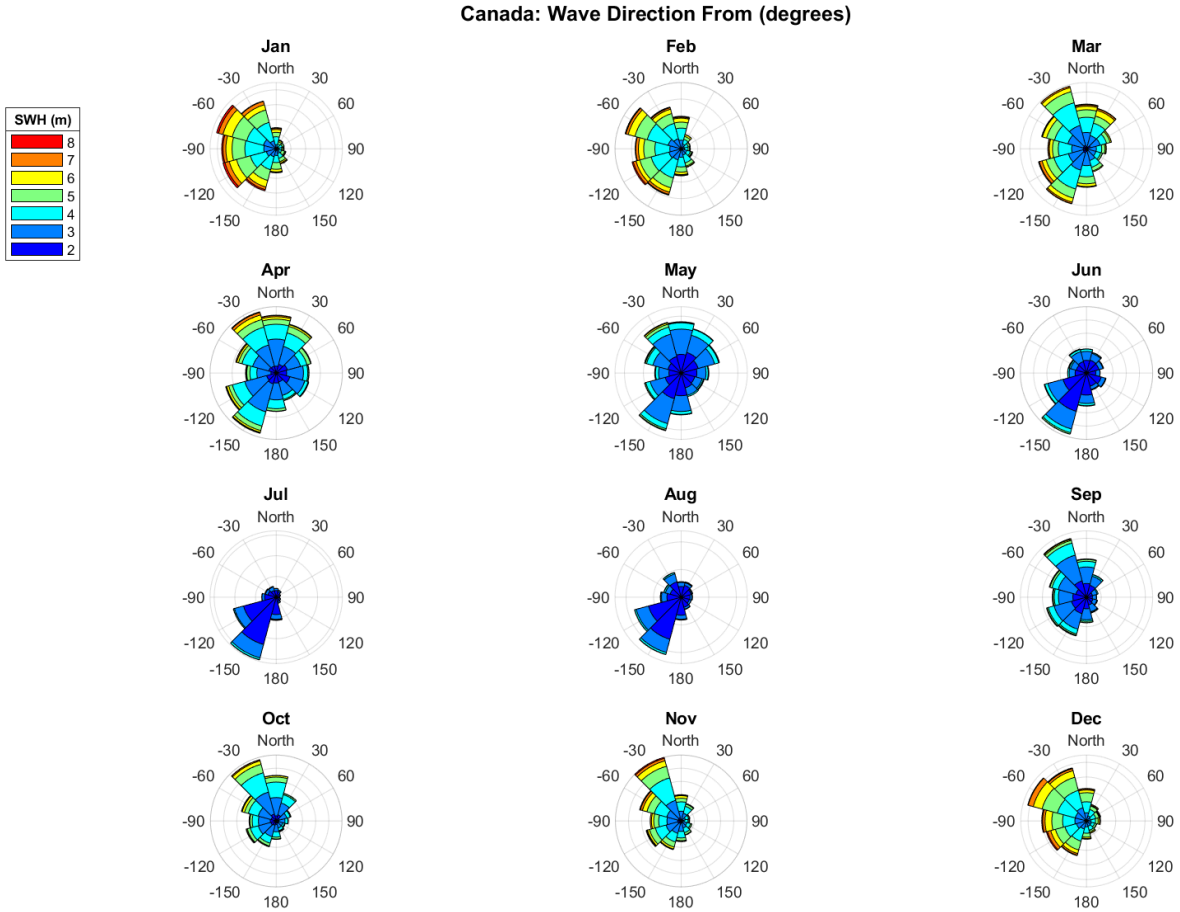

Figure 12. Monthly wind climatology for the Canadian site from the 40-year ECMWF-Interim model.

The geometry of the Norwegian site (see Figure 2) restricts the directions from which large swell can originate and this is shown by the bias of waves from the southwest (Figure 13). As with the Canadian site, there is a clear change in wave size between the Northern Hemisphere winter and summer. The largest waves during the winter (>7 m) come from the southwest from the open fetch region between Iceland and the Norwegian coast. During the summer the waves are significantly milder with few observations of significant wave height over 4 m. Mean wave directions tend to be along and slightly towards the Norwegian coast.

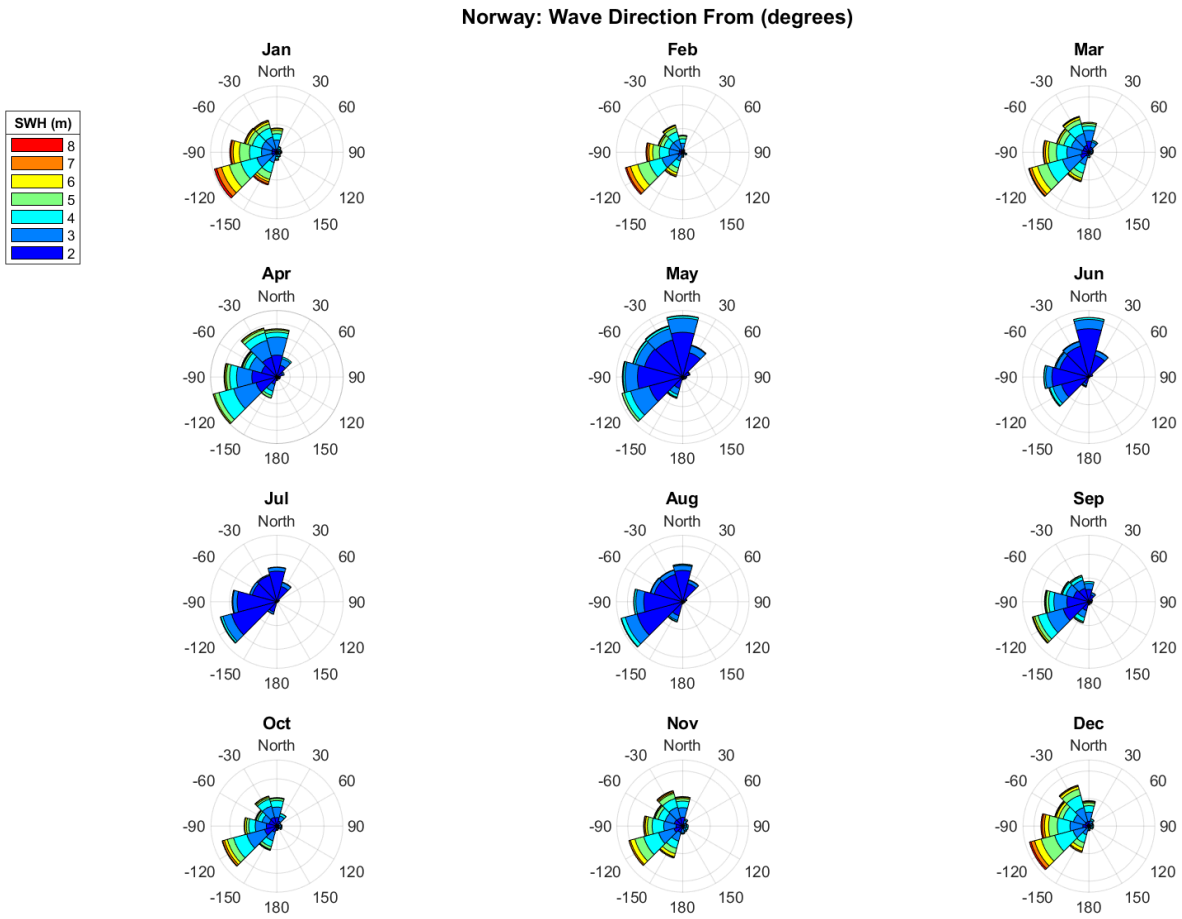

Figure 13. Monthly wind climatology for the Norwegian site from the 40-year ECMWF-Interim model.

The Brazilian wave climate is strikingly mild compared with the other three sites (Figure 14). The waves during the Southern Hemisphere summer tend to be out of the southeast with a transition to north-easterly and easterly during the winter. During all months and seasons, the significant wave height rarely exceeds 3 m. The wave directions are generally directed towards the Brazilian coast.

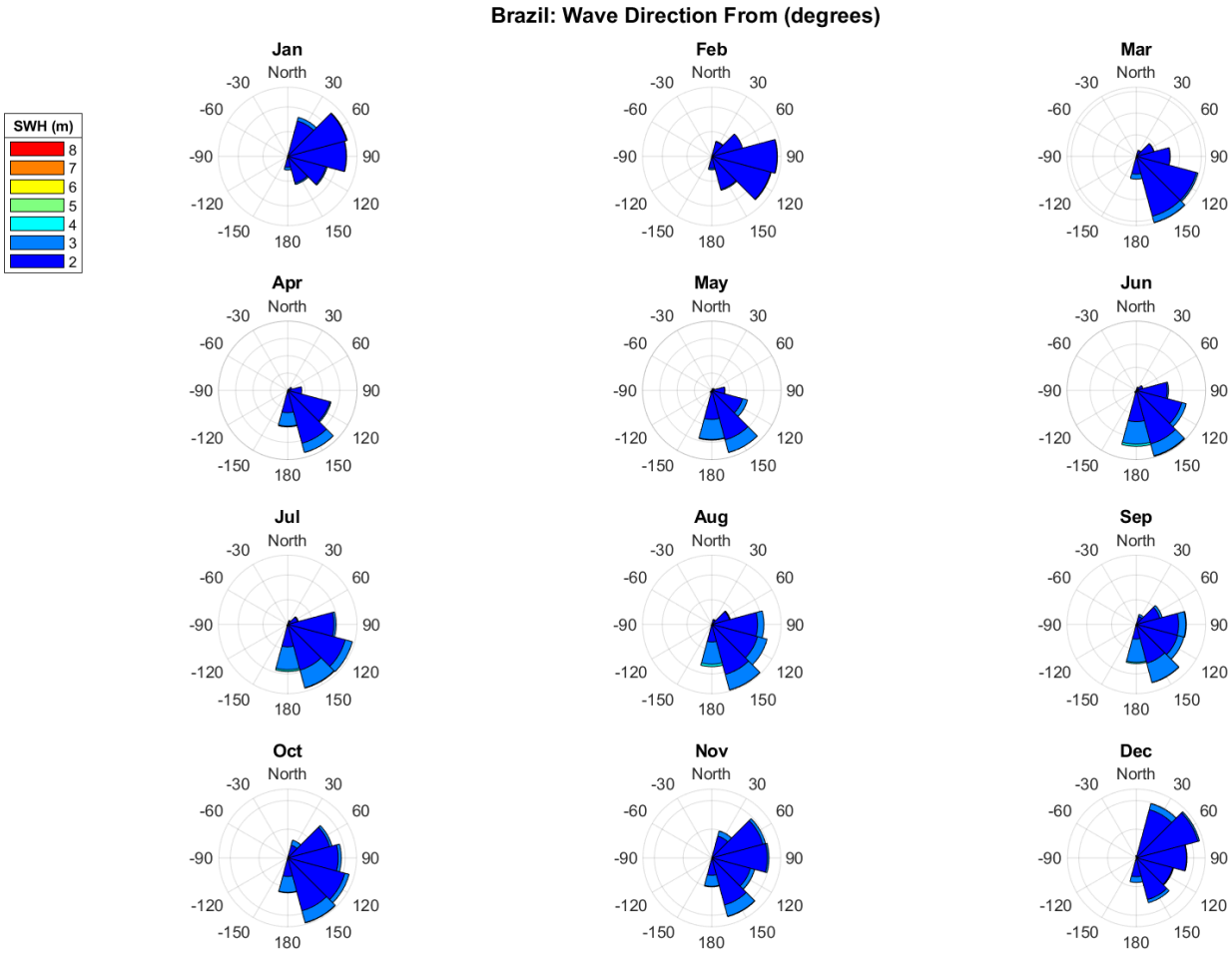

Figure 14. Monthly wind climatology for the Brazilian site from the 40-year ECMWF-Interim model.

The significant wave heights for return periods of 10, 25 and 100 years for each site (Figure 15) show the most extreme events occur in the North Atlantic, with a 100 year significant wave height of 13.3 m at the Canadian site and 14 m at the Norwegian site (Table 6). As expected from the previous analysis, the Brazilian site is not subject to large wave events, with the 100 year significant wave height (4.45 m) less than the 10 year significant wave height at any of the other sites. The GAB has a 100 year significant wave height of 10.5m.

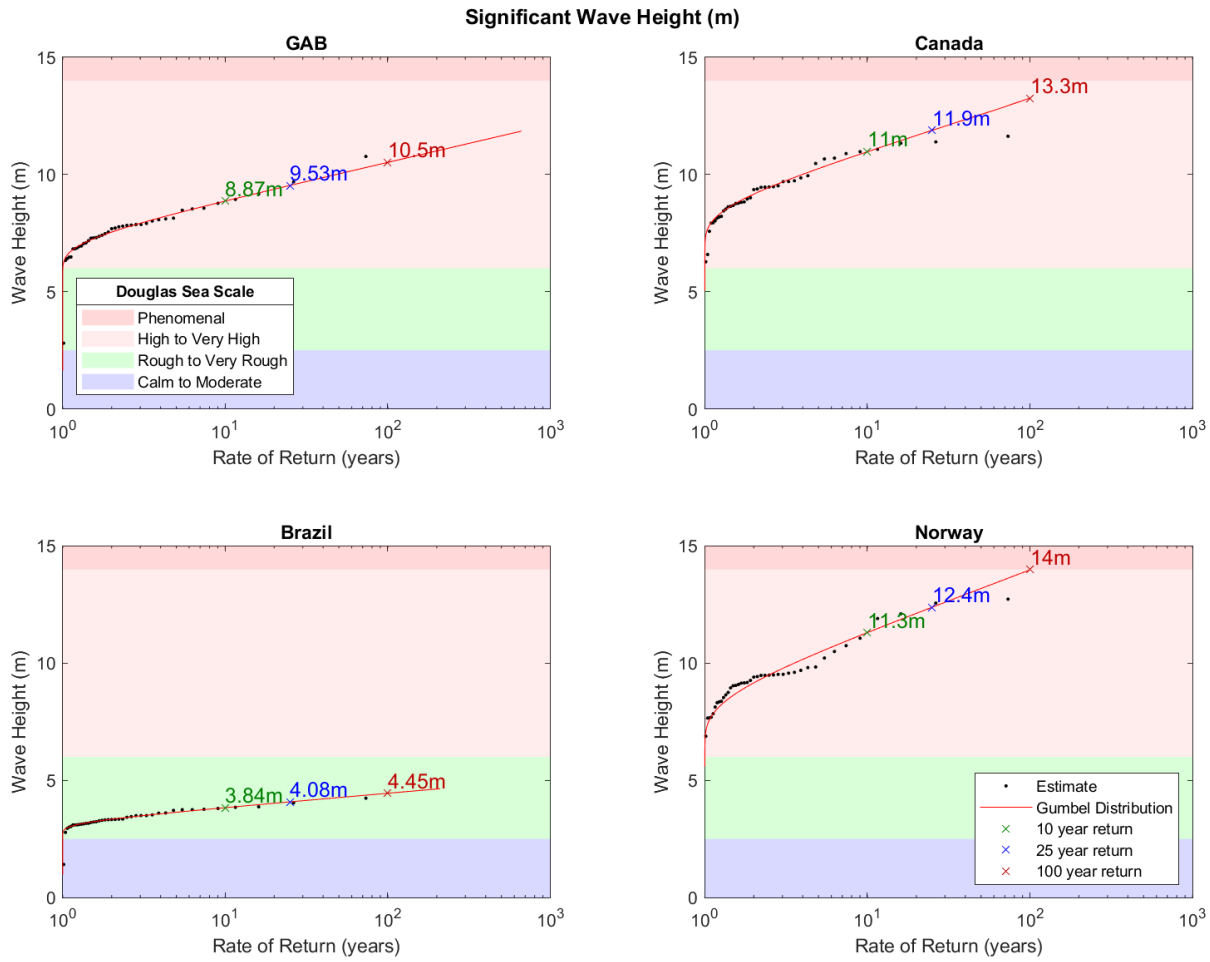

Figure 15. Significant wave height at return periods of 10, 25 and 100 years. Shading indicates corresponding Douglas Sea Scale for wave heights.

Table 7. Significant wave heights at return periods of 10, 25, and 100 years.

Return Period (years)	GAB (m)	Canada (m)	Brazil (m)	Norway (m)
10	8.9	10.9	3.8	11.3
25	9.5	11.9	4.1	12.4
100	10.5	13.3	4.5	14.0

The significant wave heights (Hs) as a function of mean wave direction are shown graphically for return periods of 10, 25 and 100 years in Figure 16. Specific values for the direction of maximum waves are presented in Table 7. In the GAB, significant wave heights greater than 5 m are expected to come from the west to south-west. Return periods in the GAB are slightly less than, but still comparable to, those expected in Canada and Norway (Table 7).

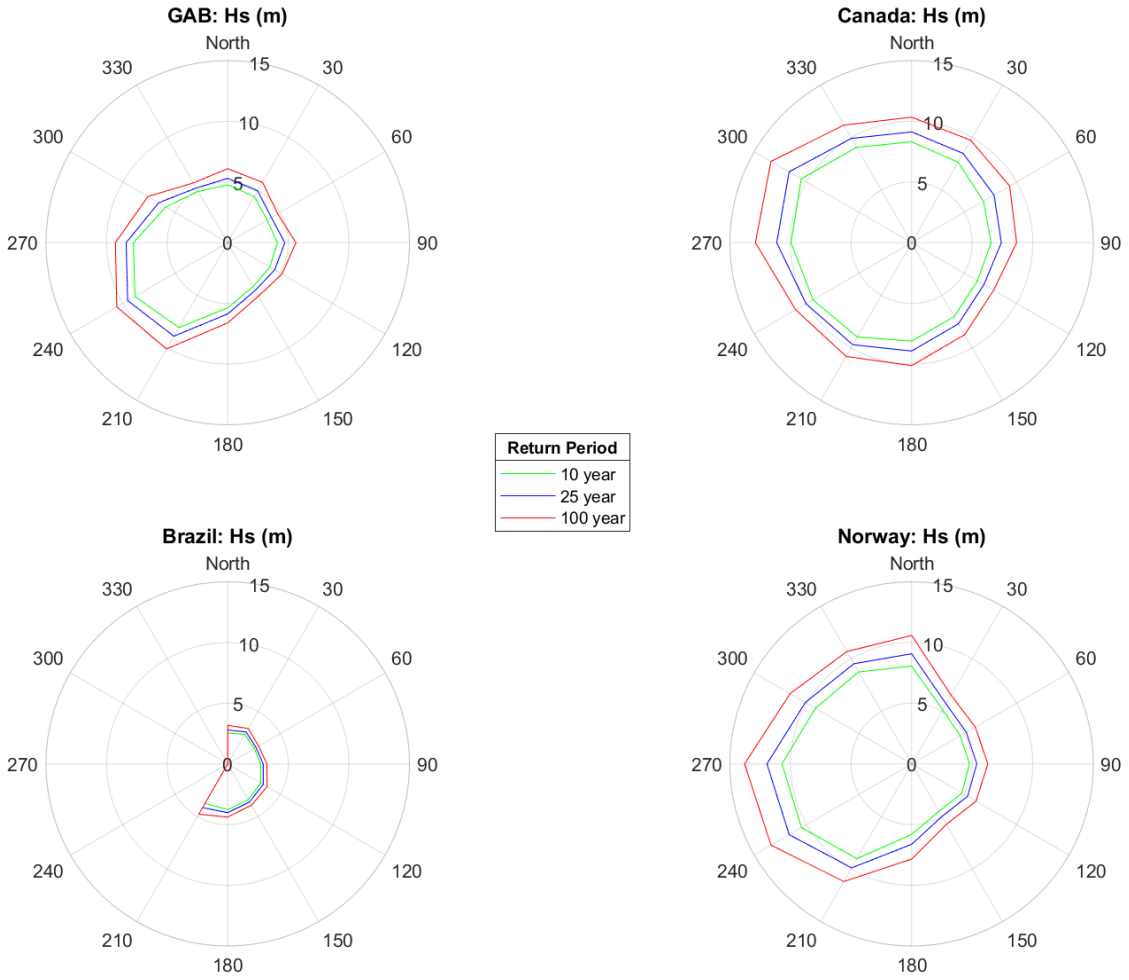

Figure 16. Signficant wave height (m) at return periods of 10, 25 and 100 years as a function of wave direction from.

Table 8. Direction of maximum significant wave heights with return periods of 10, 25, and 100 years.

	10 year		**25 year**		**100 year**	
	Direction	Hs (m)	Direction	Hs (m)	Direction	Hs (m)
GAB	-120	8.84	-120	9.54	-120	10.57
Canada	-60	10.52	-60	11.67	-60	13.40
Brazil	180	3.77	-150	4.15	-150	4.78
Norway	-90	10.70	-90	11.94	-90	13.78

Maximum wave heights (Hmax) are encountered infrequently and are generally produced by waves interacting from multiple directions. Estimates based on the spectrum satisfying a Rayleigh distribution suggest that the maximum wave height would be measured no more than 3 times a day. Estimates of maximum wave height are still important for engineering purposes, so the climatological return period analysis for each of the locations is shown in Figure 17. For the four sites, the results are similar to the results for Hs (Figure 15), with the North Atlantic sites have the largest Hmax values and Brazil having the smallest. One exception is that the Canadian site shows a larger Hmax at each return period than the Norwegian sites while the reverse was true for Hs. It should be noted that the Hmax predictions from the ECMW CERA-20 model are on a different resolution grid to the ERA-Interim model, and consequently the Norwegian and Canadian Hs calculation sites are slightly displaced from site location used for the Hmax calculation. However, the Hmax dynamics are more complex than the Hs dynamics, so this may reflect a real difference.

The return periods of the maximum wave height for each location are presented in Table 8. Consistent with the climatological analysis (Figure 10), the extreme wave events in the GAB site are from the same sector (southwest and directed onshore) for all return periods. For the Canadian site, the extreme waves are also all from the same sector, slightly from the northwest and directed offshore. The Brazilian extreme waves are more variable in direction depending on return period, but the extreme events are quite moderate compared to other sites, and all wave directions are off-shore. The Norwegian site, again, shows the largest extreme significant wave heights, with the predominant direction from due west. For the Norwegian site this suggests extreme wave events move in the or onshore.

Table 9. Maximum wave heights at return periods of 10, 25, and 100 years.

Return Period (years)	GAB (m)	Canada (m)	Brazil (m)	Norway (m)
10	14.2	21.4	7.1	19.3
25	15.5	23.1	7.5	21.1
100	17.4	25.8	8.1	23.7

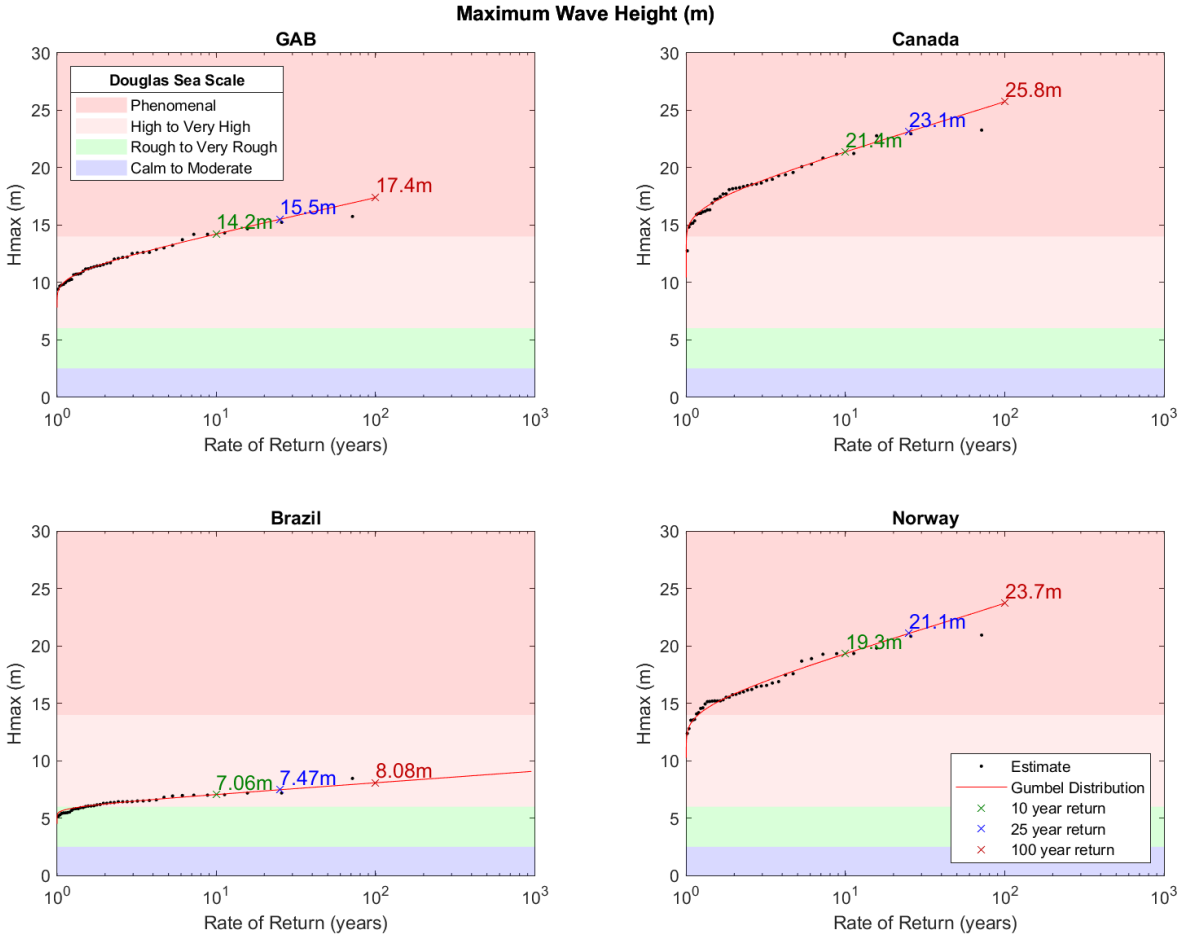

Figure 17. Maximum wave height at return periods of 10, 25 and 100 years. Shading indicates corresponding Douglas Sea Scale for wave heights.

Wave period is generally positively correlated with Hs. Larger waves tend to have longer periods, and ocean swell generally has periods greater than 10 seconds. Large waves with short periods tend to become too steep to persist and this results in wave breaking and energy dissipation. Calculations show little variation between 10 year and 100 year return periods for wave period at each site (Figure 18), with about a half second range in the GAB and less than 2 sec at the more variable sites (Table 10). This suggests persistent swell conditions at all sites.

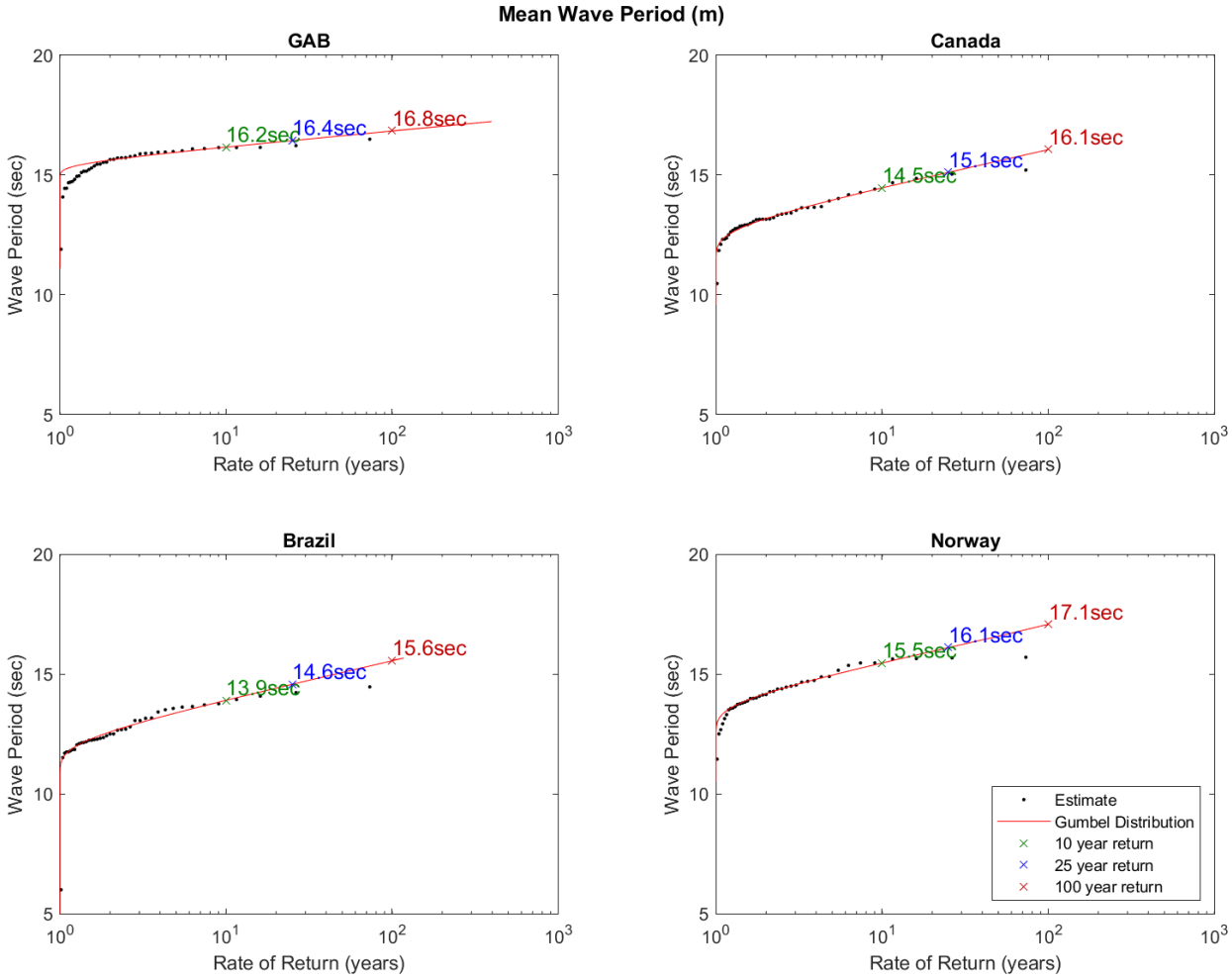

Figure 18. Mean wave period at return periods of 10, 25 and 100 years.

Table 10. Mean wave period at return periods of 10, 25, and 100 years.

Return Period (years)	GAB (sec)	Canada (sec)	Brazil (sec)	Norway (sec)
10	16.2	14.5	13.9	15.5
25	16.4	15.1	14.6	16.1
100	16.8	16.1	15.6	17.1

The wave climate at each of the sites is summarized with the 10 year CAWCR spectral model output. The power spectrum, as a function of wave period and direction, is shown in Figure 19. Consistent with the directional information from wave heights (Figure 9), the directional spectra for mean wave period show that the GAB site is subject to an extremely consistent strong swell (period > 10 sec) from out of the southwest. The Canadian site shows a more multidirectional swell signature while the Brazilian site shows waves coming persistently from the southeast. The Norwegian site shows a moderately strong signal from west-southwest but

also energy propagating in from a relatively wide band from the northwest. The variety of directions from which energy propagates into the North Atlantic sites may also explain why Hmax values are so much higher at these sites.

The peak wave period is shown more clearly in the directionally integrated wave spectra (Figure 20). The GAB, Canadian, and Norwegian sites show strong swell signals, with the GAB having a sharper profile and peak power (i.e. energy) at a slightly longer period than the other two sites. This is consistent with the swell in the GAB having a more persistent origin in the Southern Ocean. The Canadian site is more energetic overall, with the greatest overall integrated power. The Brazilian site, in contrast, is a relatively low energy environment, dominated by short period waves commonly associated with local winds.

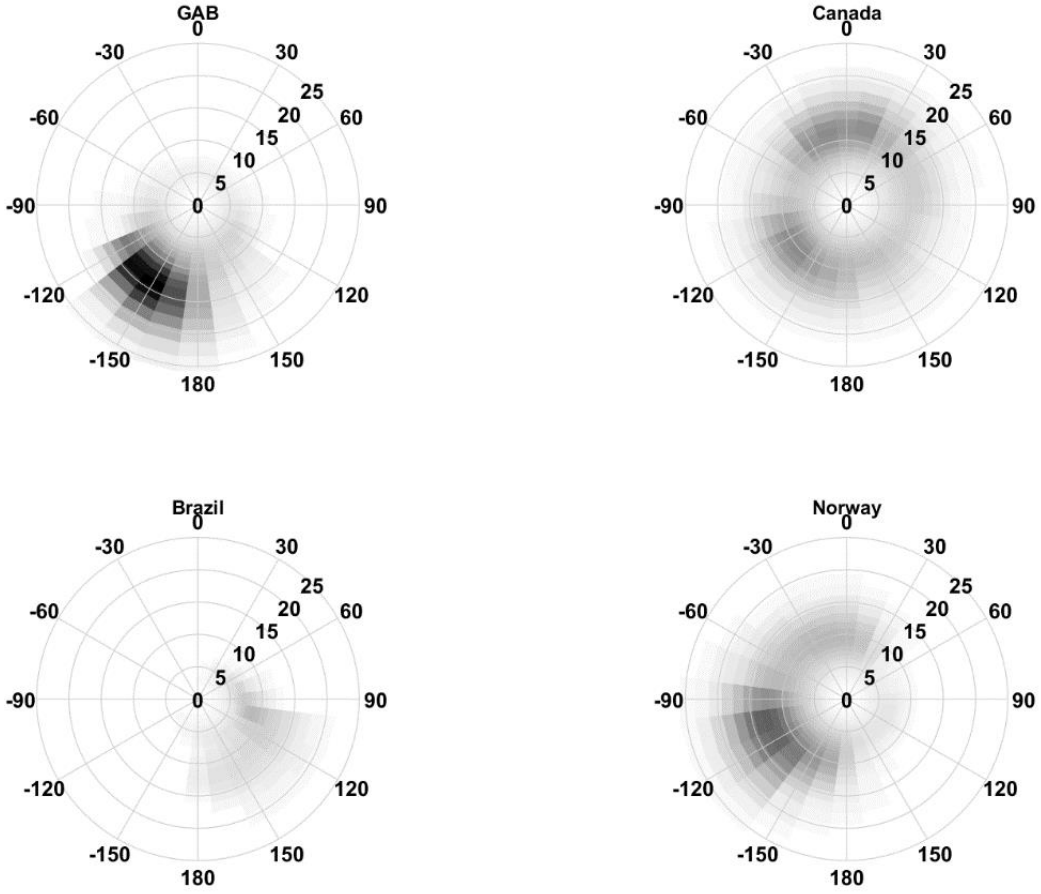

Figure 19. Wave spectra as a function of direction and wave period. All spectra are plotted on the same intensity scale, with darker shading representing more power at that period in that sector.

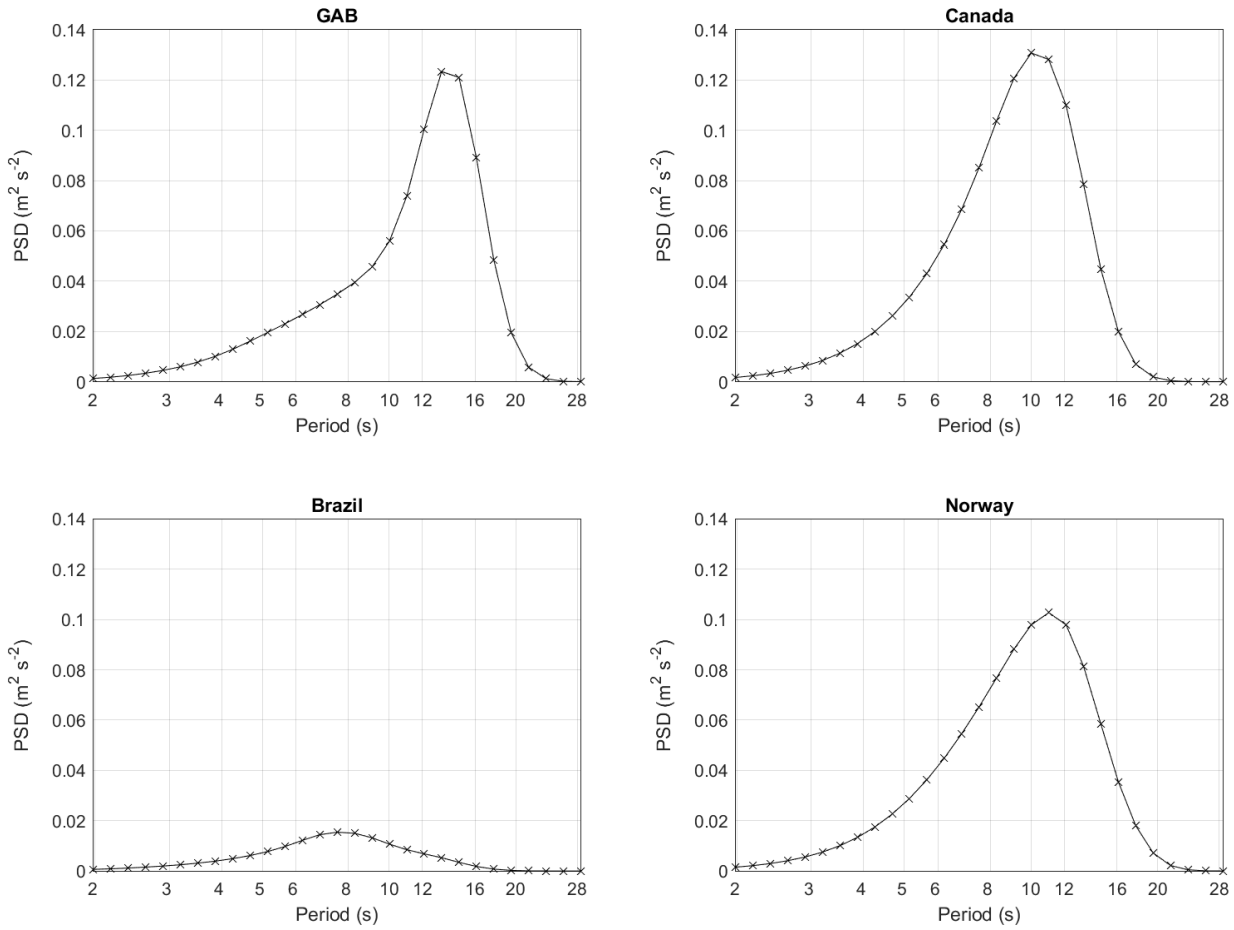

Figure 20. Directionally integrated power spectral density (PSD) as a function of wave period at each site. The PSD is plotted in power preserving format with the area under the curve corresponding to the relative power at that frequency or period.

Wave Trends

Trends from 2008 to 2018 for significant wave height (Hs) are shown for each location in Figures 21-24. Significant wave height trends by months in the GAB showed significant ($p < 0.1$) increases in Hs during February and July, with a maximum growth rate of 9.2 cm/year in July (Figure 21). Collectively, 7 months showed a growing trend and 5 months showed a decreasing trend.

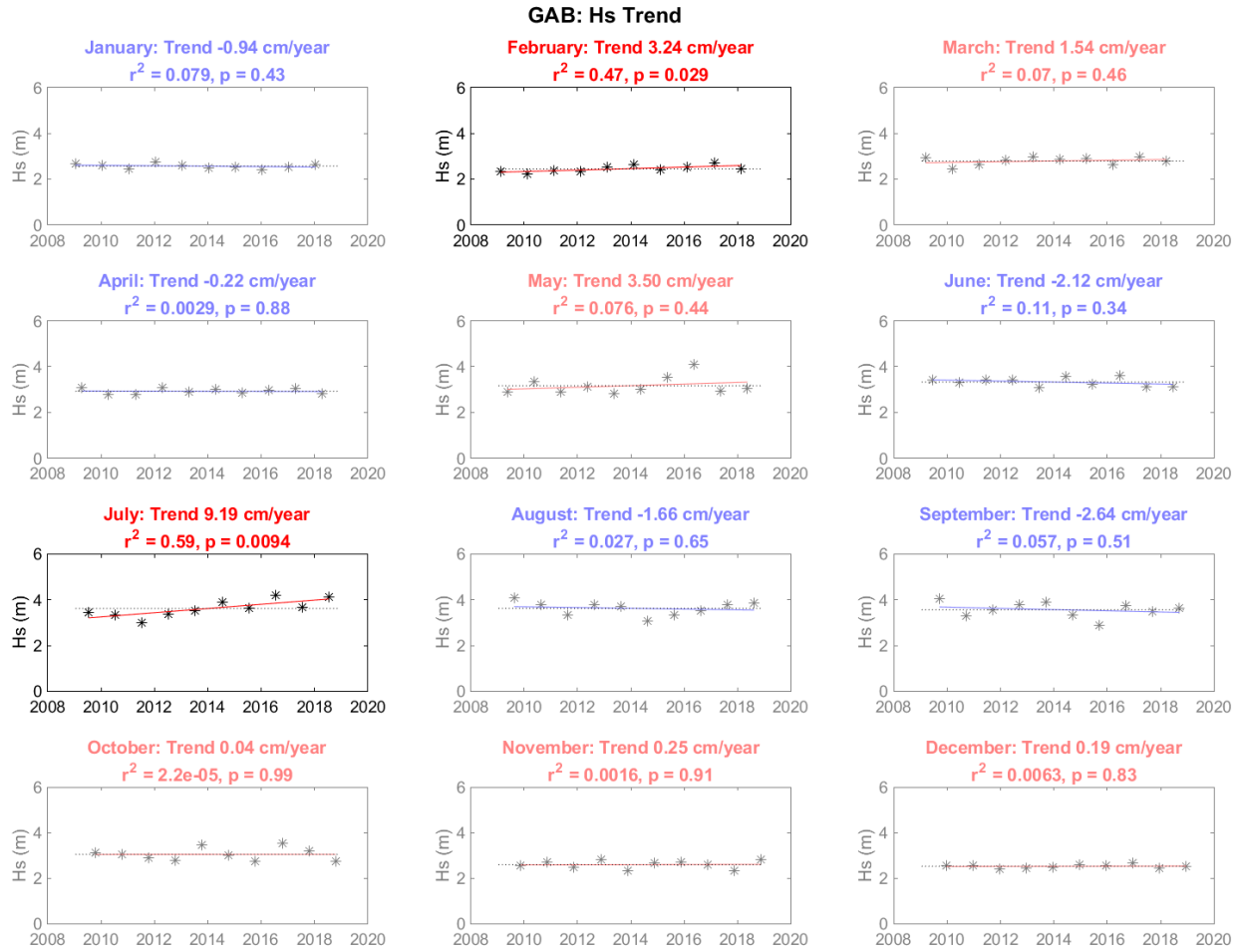

Figure 21. GAB monthly significant wave height trends from 2008 to 2018. Positive trends are indicated in red. Correlation is represented by r^2 and significance is presented as values of p where (1-p)*100% is the confidence level for a significant trend. Months for which the confidence level was less than 90% ($p > 0.1$) are shaded out.

For the Canadian site there were two months with significant trends, with Hs decreasing in January and October over the last 11 years (Figure 22).

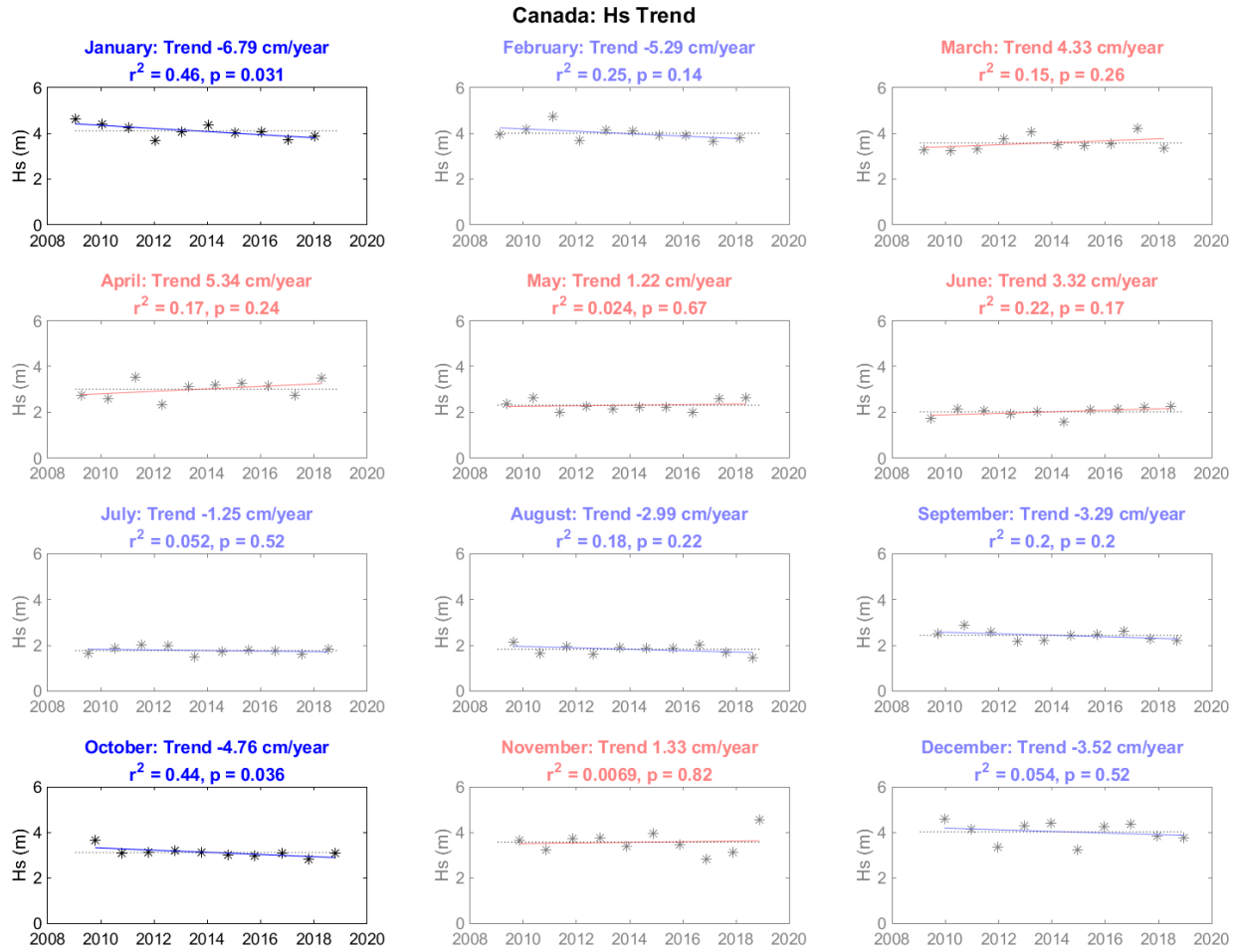

Figure 22. Canadian monthly significant wave height trends from 2008 to 2018. Positive trends are indicated in red. Correlation is represented by r^2 and significance is presented as values of p where (1-p)*100% is the confidence level for a significant trend. Months for which the confidence level was less than 90% (p >0.1) are shaded out

For the Norwegian site, only July showed a significant decreasing trend in significant wave height over the last 11 years (Figure 23).

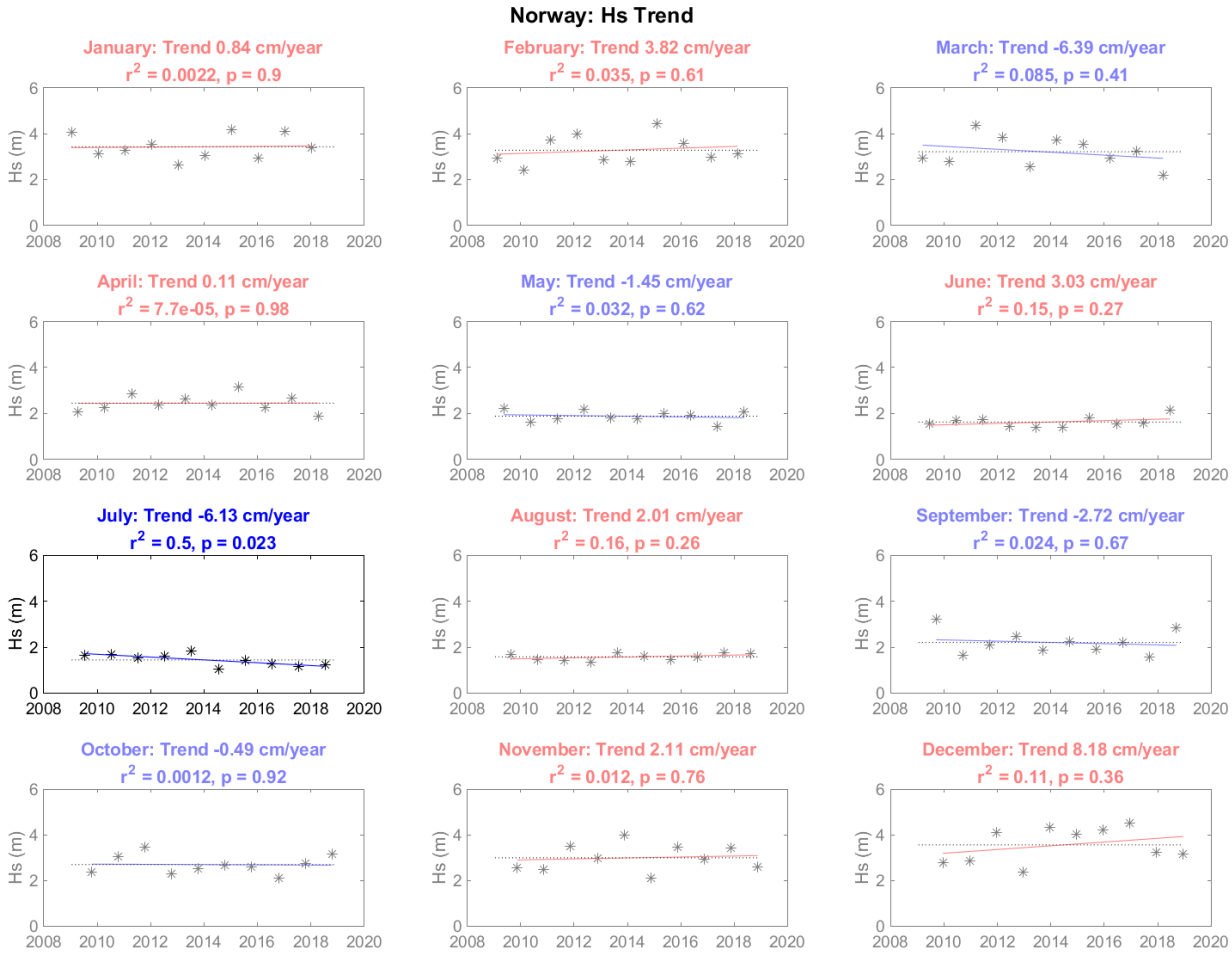

Figure 23. Norwegian monthly significant wave height trends from 2008 to 2018. Positive trends are indicated in red. Correlation is represented by r^2 and significance is presented as values of p where (1-p)*100% is the confidence level for a significant trend. Months for which the confidence level was less than 90% (p >0.1) are shaded out.

The Brazilian site showed no trends in significant wave height (Figure 24).

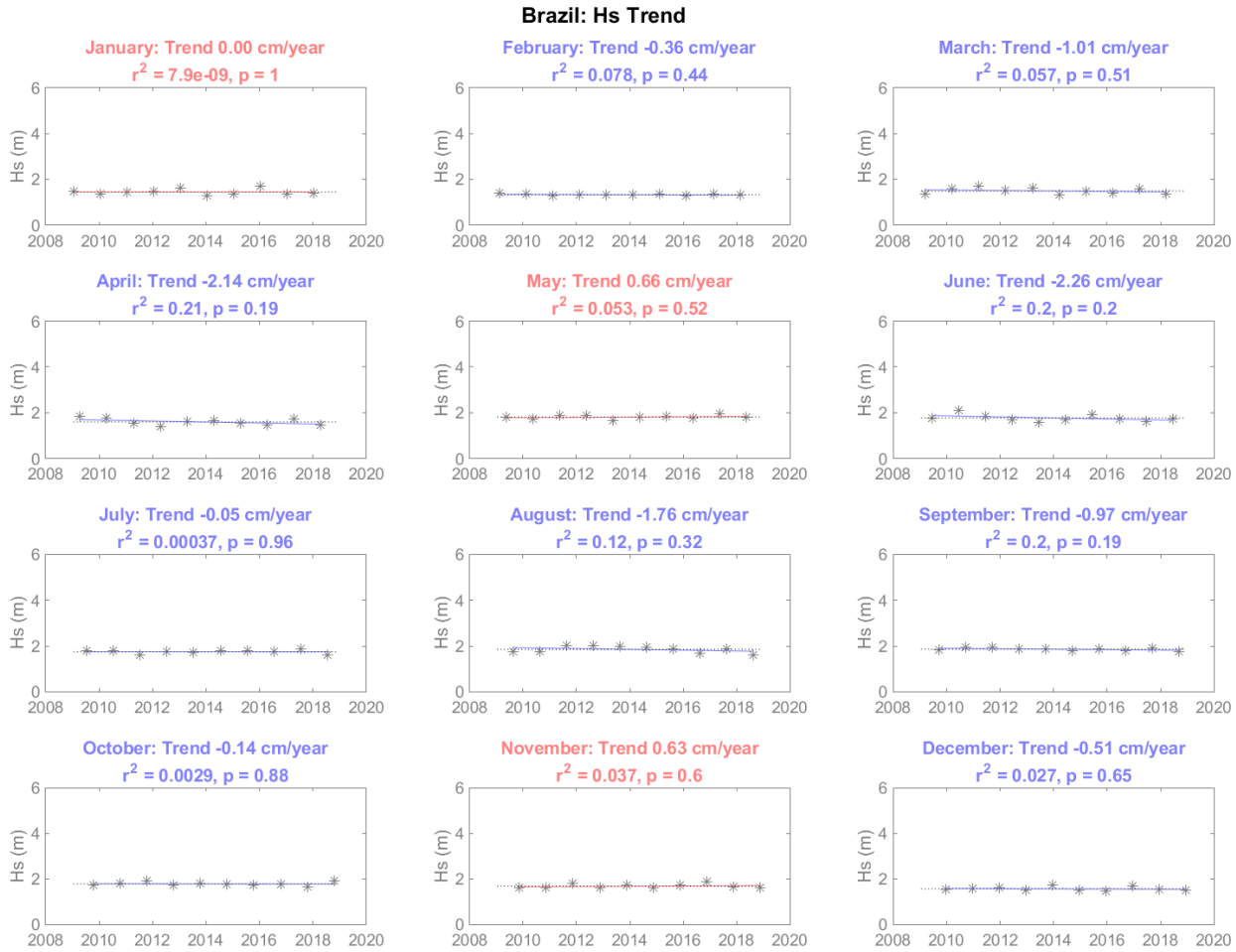

Figure 24. Brazilian monthly significant wave height trends from 2008 to 2018. Positive trends are indicated in red. Correlation is represented by r^2 and significance is presented as values of p where (1-p)*100% is the confidence level for a significant trend. Months for which the confidence level was less than 90% (p >0.1) are shaded out.

Trends in maximum wave heights (Hmax) over the last 11 years for each location are shown in Figures 25-28. In general, across this period the trends were weak with few trends significant at the 90% confidence level (p <0.1). At the GAB site all but two months (June and September) showed increases in maximum wave height (Figure 25). Three months (February, April and July) showed a significant (p <0.1) increase in Hmax, with the strongest increase of over 19 cm/year occurring in July.

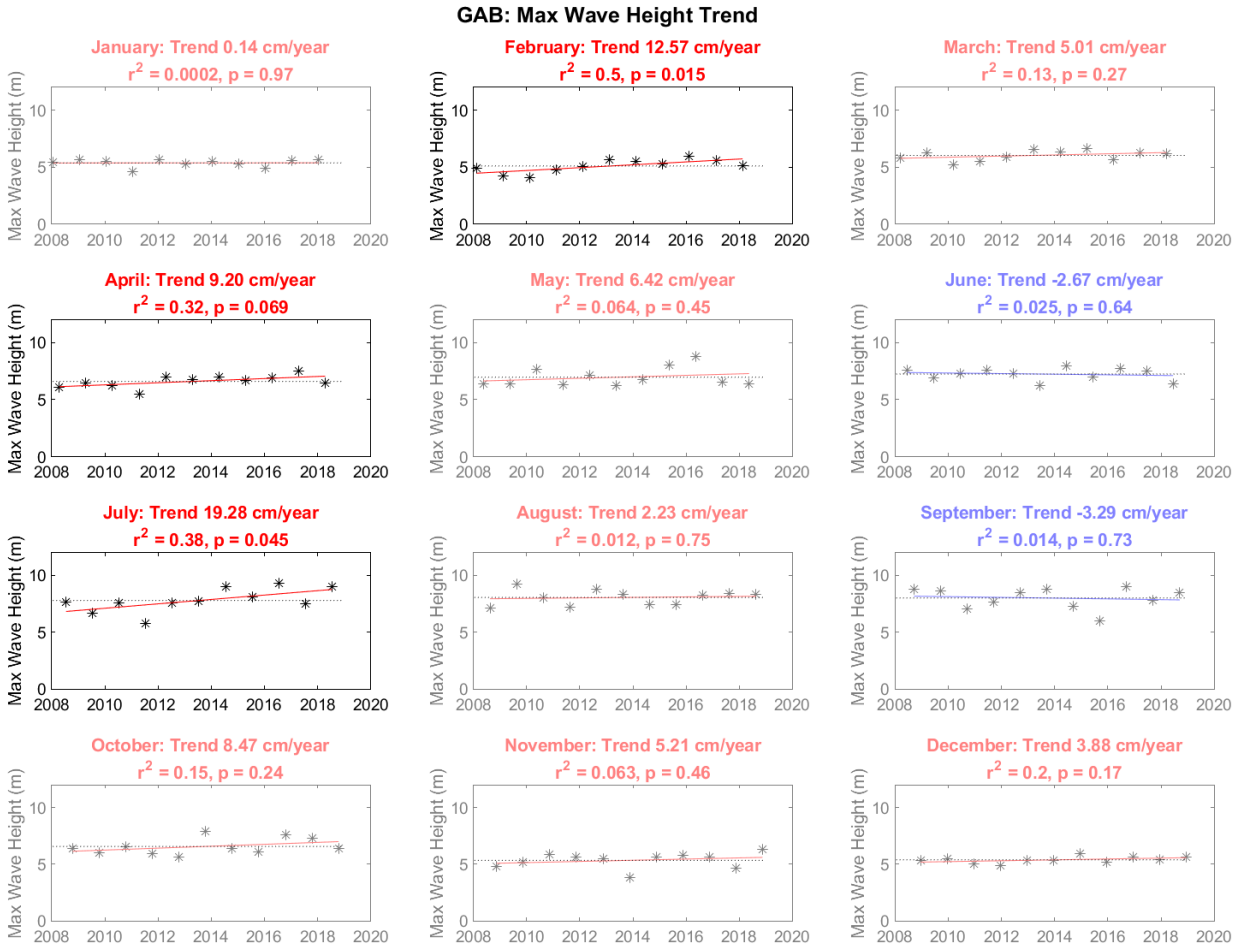

Figure 25. GAB monthly-maximum wave height trends from 2008 to 2018. Positive trends are indicated in red. Correlation is represented by r^2 and significance is presented as values of p where (1-p)*100% is the confidence level for a significant trend. Months for which the confidence level was less than 90% (p >0.1) are shaded out.

Trend analysis for maximum wave height at the Canadian is shown in Figure 26. There were no months for which the trend was considered significant at the 90% confidence level.

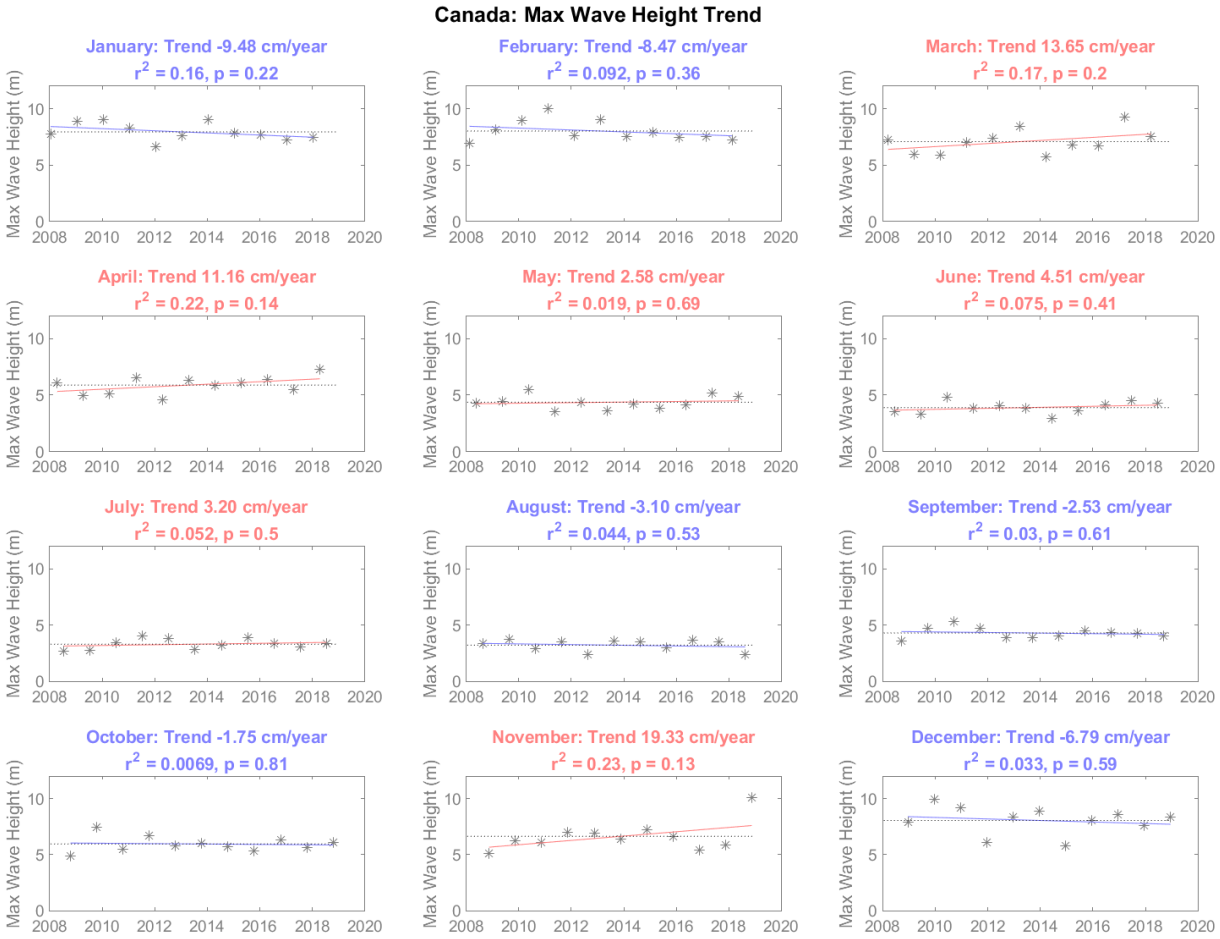

Figure 26. Canadian monthly-maximum wave height trends from 2008 to 2018. Positive trends are indicated in red. Correlation is represented by r^2 and significance is presented as values of p where (1-p)*100% is the confidence level for a significant trend. Months for which the confidence level was less than 90% (p >0.1) are shaded out.

For the Norwegian site, only August had a significant trend, with a rate of maximum wave height increase of 10.9 cm/year (Figure 27). Across the year, eight out 12 months showed positive trends.

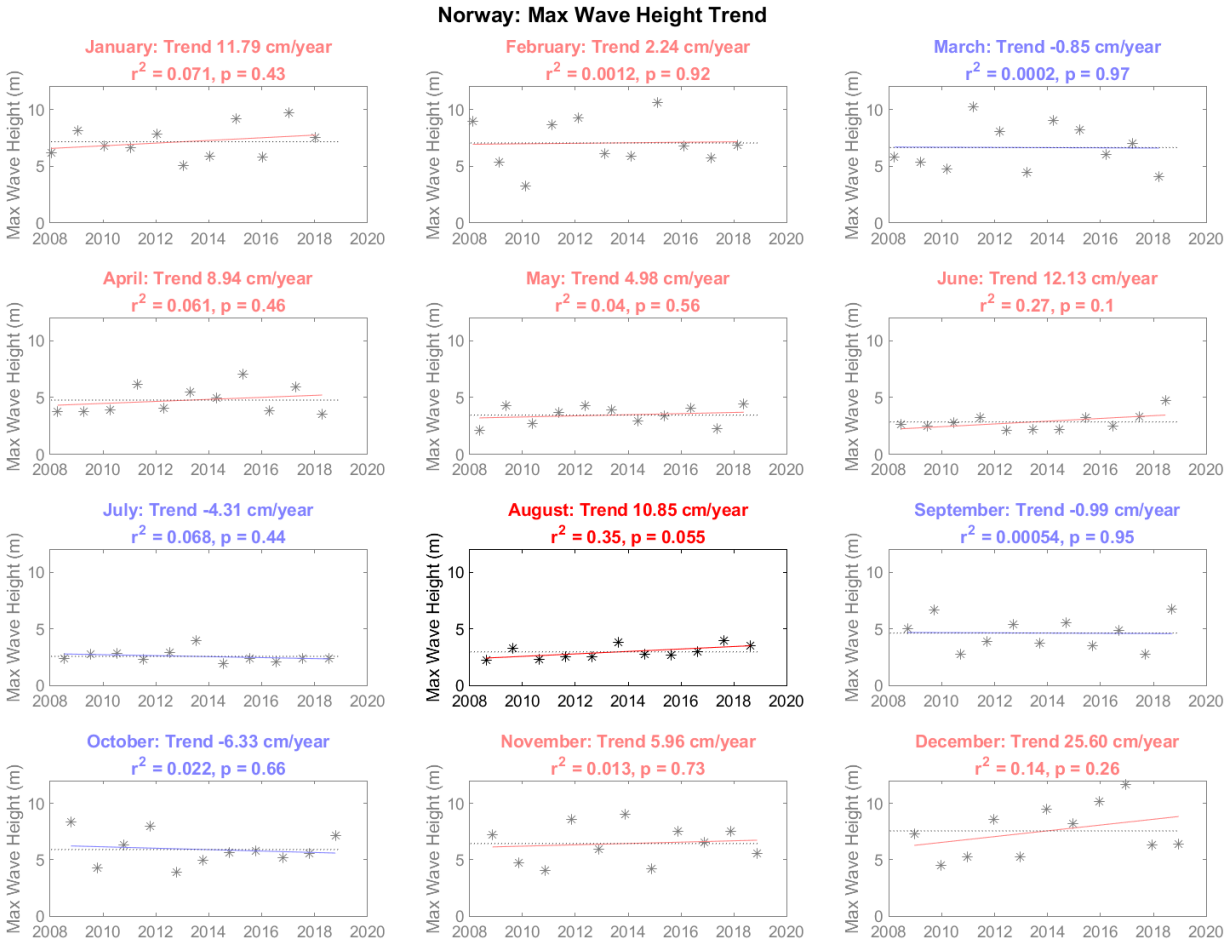

Figure 27. Norwegian monthly-maximum wave height trends from 2008 to 2018. Positive trends are indicated in red. Correlation is represented by r^2 and significance is presented as values of p where (1-p)*100% is the confidence level for a significant trend. Months for which the confidence level was less than 90% (p >0.1) are shaded out.

Trend analysis at the Brazilian showed no significant trends, although there were a majority of months for which the slope of the trend was near zero or negative indicating no significant change in the maximum wave heights experienced each month over the last 11 years (Figure 28).

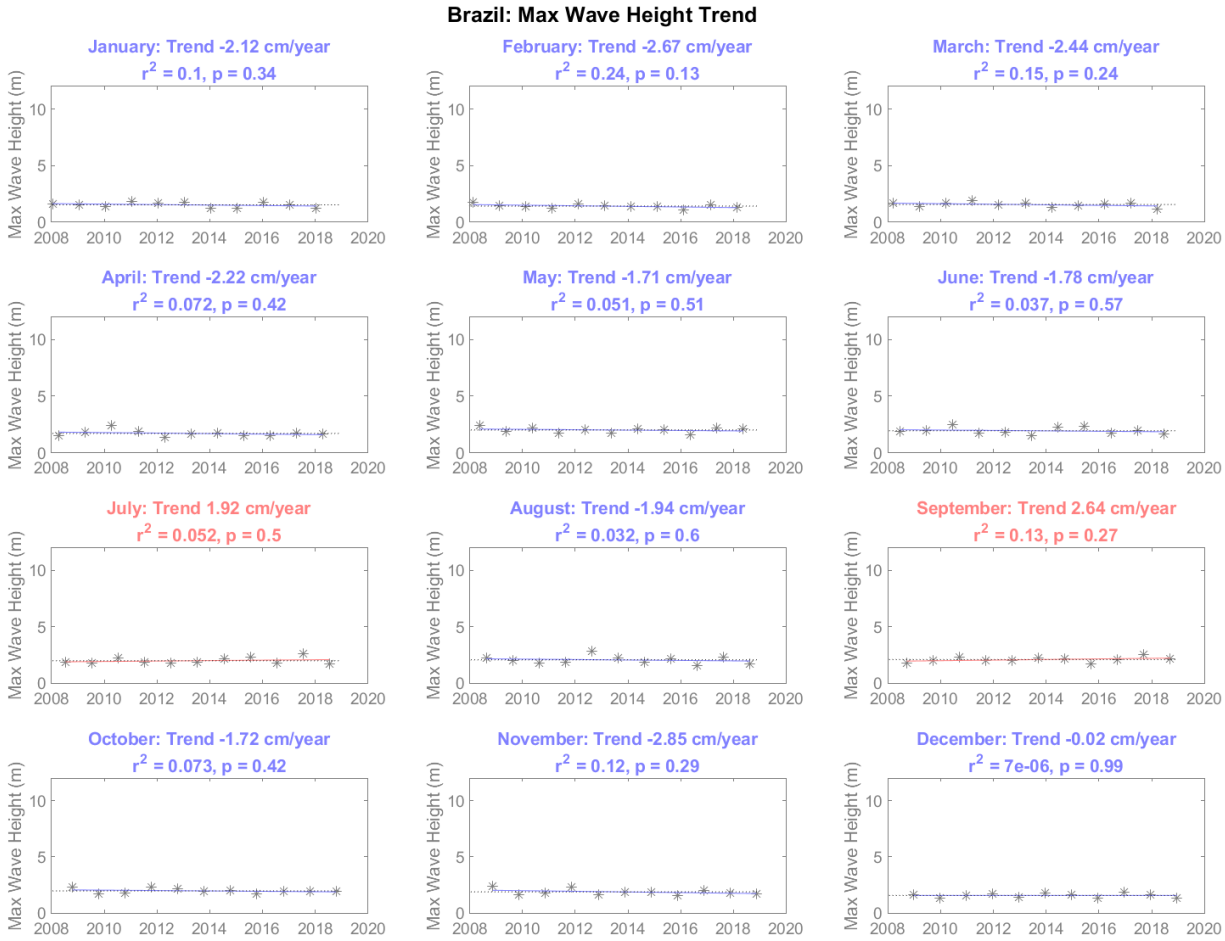

Figure 28. Brazilian monthly-maximum wave height trends from 2008 to 2018. Positive trends are indicated in red. Correlation is represented by r^2 and significance is presented as values of p where (1-p)*100% is the confidence level for a significant trend. Months for which the confidence level was less than 90% (p >0.1) are shaded out.

Currents

Eleven years of BRAN model data from 2009-2019 have been temporally averaged over three depth ranges to indicate long term trends in current speed and directions for each location (Figures 29-31). In the top 50 m (Figure 29), the strongest currents were observed heading to the southwest at the Brazil site. Surface Currents were quite directional at the Canadian and Brazilian sites, with wider variation in current directions at the Norway and GAB sites. In the GAB, dominant average current speeds of up to 30 cm/s were directed from the northeast and southeast, indicating a predominantly alongshore flow in the surface 50 m of the water column.

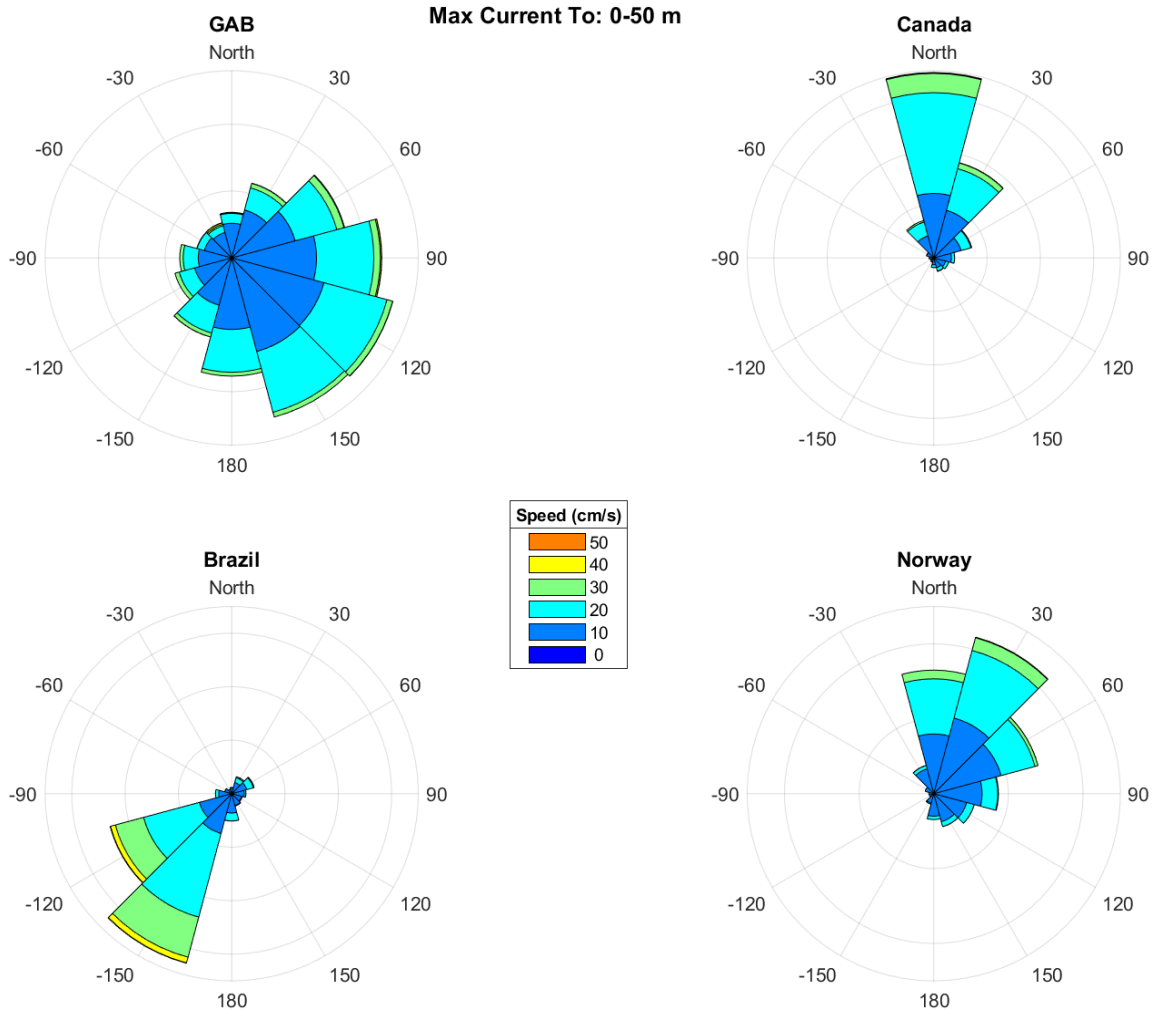

Figure 29. Circular histograms of BRAN model current speed and direction at the four sites averaged over 11 years and 0-50 m depth.

In the depth range from 50-200 m (Figure 30), currents at the Brazilian site showed the largest change in direction compared to the flow direction shown in the surface 50 m layer. This would imply a strong vertical shear in the residual circulation. At the other sites, the flow is generally in the same direction as the surface currents, but with a slight weakening in amplitude. In the

GAB, compared to currents in the surface 50 m, currents between 50-200m showed less variability in direction and were predominantly from the southeast.

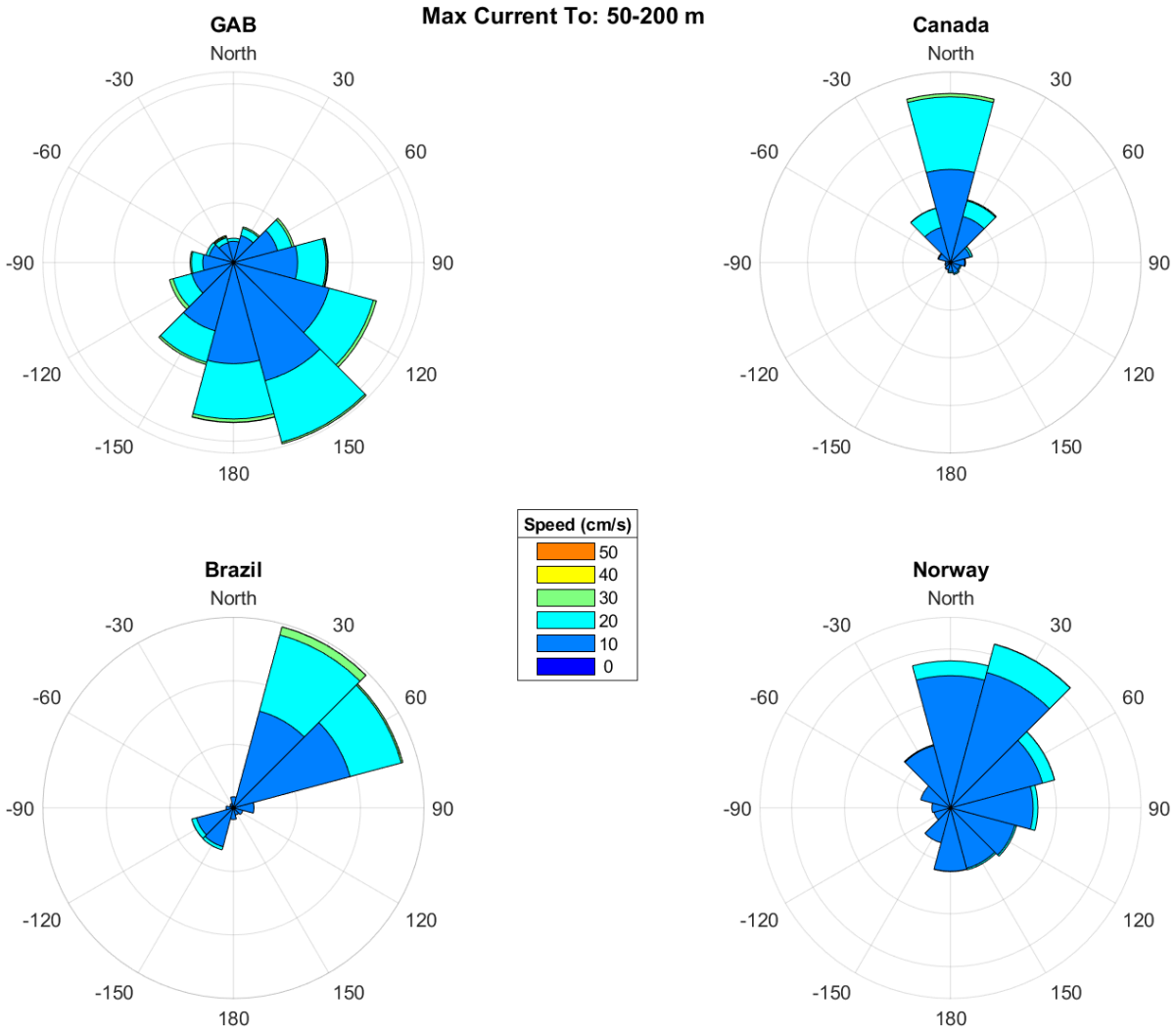

Figure 30. Circular histograms of BRAN model current speed and direction at the four sites averaged over 11 years and 50-200m depth.

Deeper water current speeds and directions averaged across depths below 200m are shown in Figure 31. Compared to the surface flows, the largest direction changed occurred at the GAB site, with current flows towards the northeast to east with maximum speeds of 20 cm/s, suggesting a degree of shear and upwelling towards and onto the shelf. The velocities at the other sites are generally weaker but in the same direction as for the 50-200 m depth range.

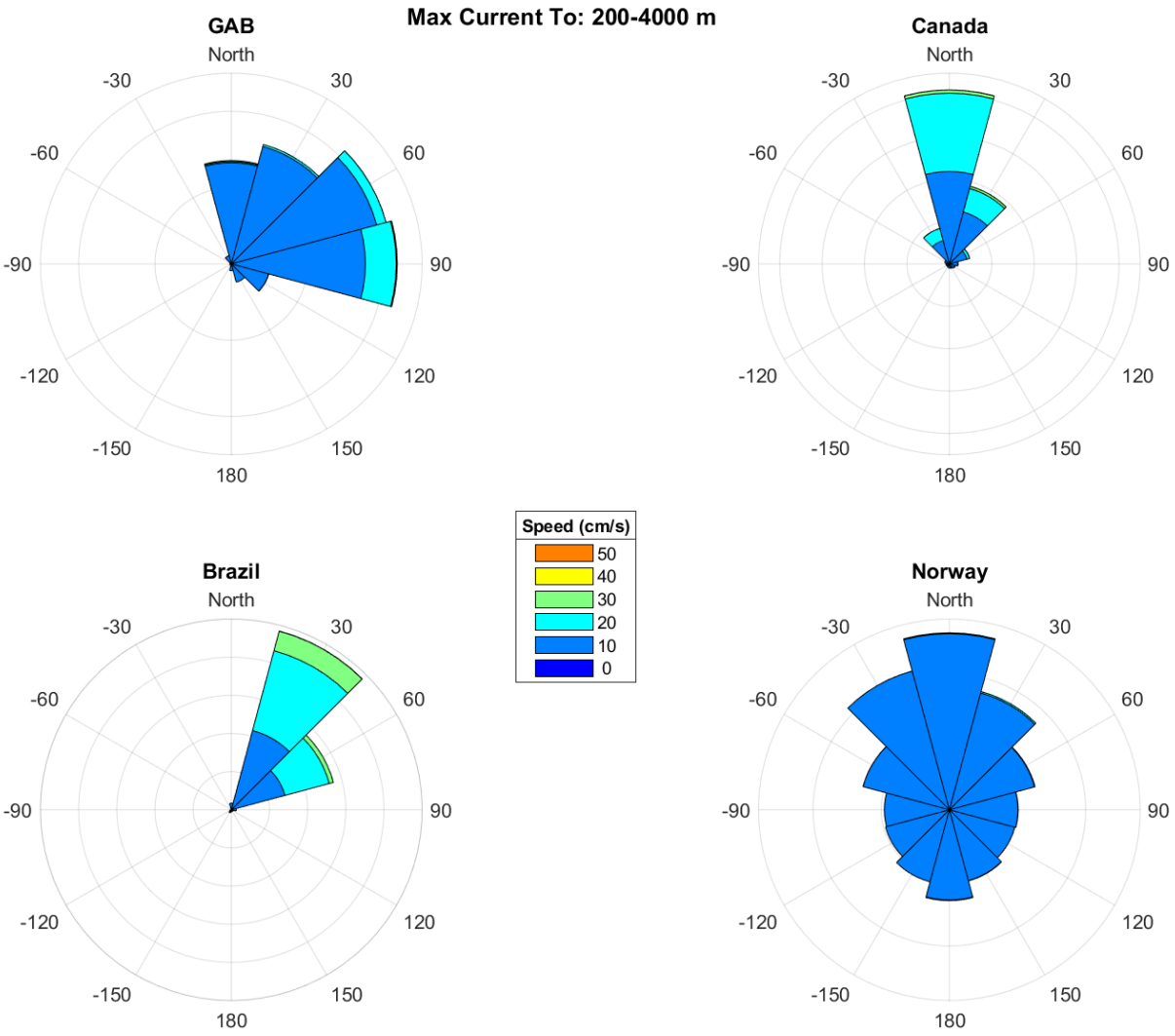

Figure 31. Circular histograms of BRAN model current speed and direction at the four sites averaged over 11 years and 200-4000 m depth.

Comparison of 2008-2012 wind and wave environment to climatological mean

A comparison between the monthly average wind and wave conditions experienced across the 2008-12 period with the long term (40 year) climatological mean for the GAB is shown in Figure 32. Monthly averages for both significant wave height (Hs) and 10 m wind speed remained within a standard deviation of the 40 year average.

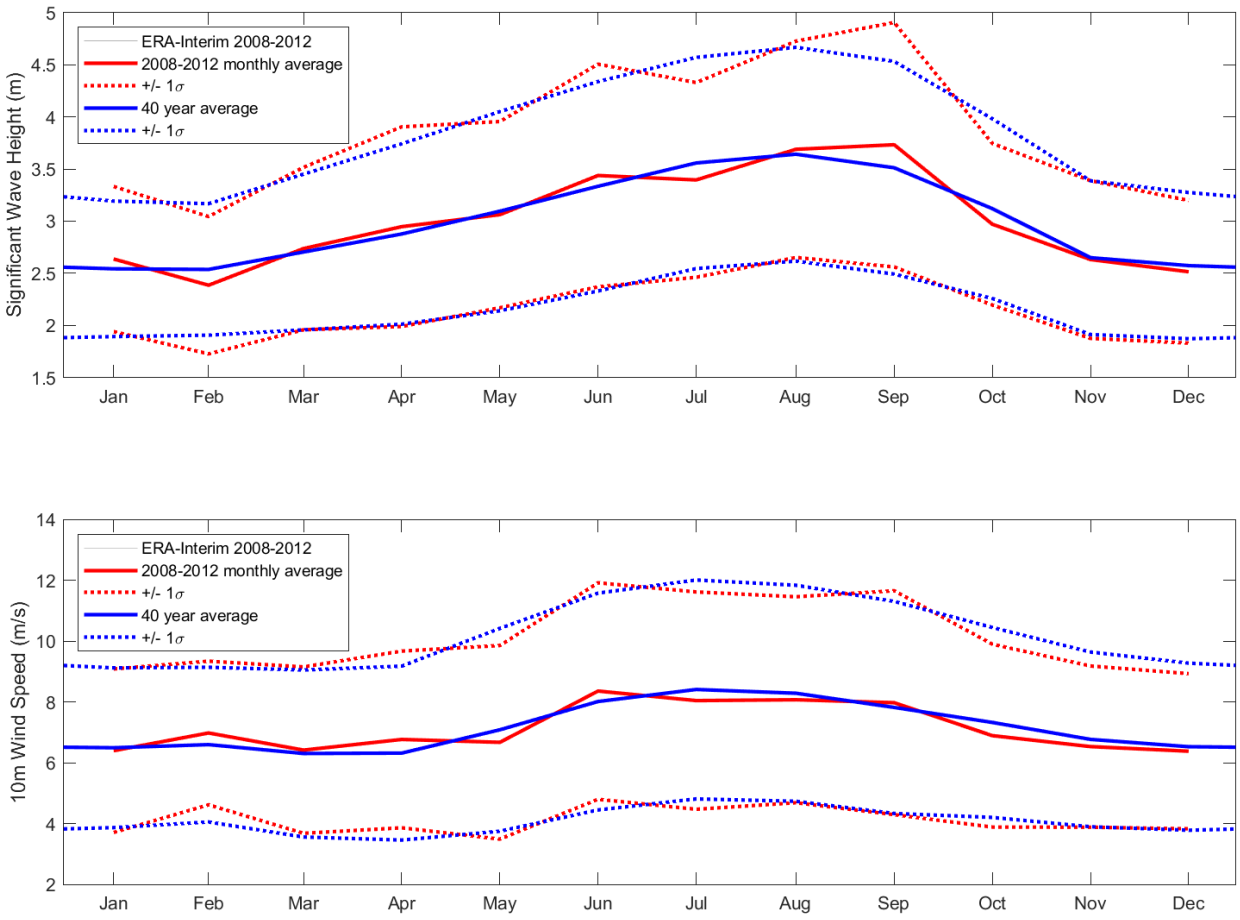

Figure 32. Comparison of average wave and wind conditions for 2008-2012 period with the long term (1979-2018) climatological averages and standard deviations.

Wave and wind sea state thresholds

Analysis of periods of five consecutive days or more below a significant wave height (Hs) ranging from slight (<1.5 m) to rough (<4.5 m) for each location is shown in Figure 33. At the GAB site, during the 40-year period of the ERA-interim output, there was only a single event where Hs was continuously below 1.5 m for 5 days, effectively 0.0% of the record length. There were relatively few periods (<10% of the time) where Hs was below 2.5 m. At the Canadian site Hs was only below 1.5 m for approximately 2% of the time, however, about a quarter of the time (26%) Hs was below 2.5 m. Due to the milder wave climate at the Brazilian site, Hs was almost always (95%) below 2.5 m and below 1.5 m for over 22% of the time. Despite being exposed to frequent severe weather events, the Norwegian site still had consecutive days of Hs below 2.5 m for over 40% of the time and below 1.5 m more that 10% of the time.

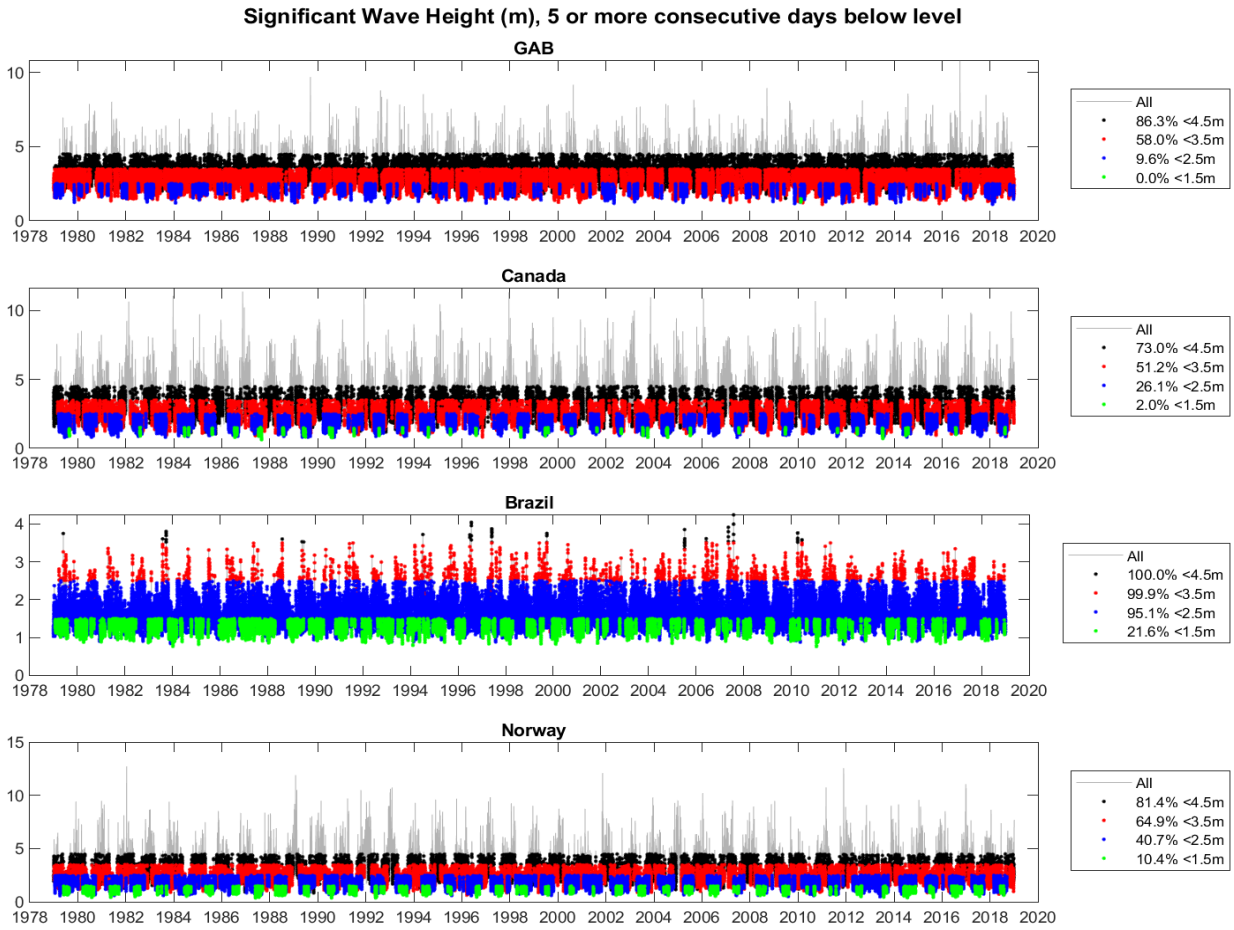

Figure 33. Full 40-year Hs model output for all four sites, highlighting, by colour, periods of 5 or more days below the specified significant wavehight threshold. The percentage of time as a function of the entire record where these conditions were met are summarized next to each time series.

Figure 34 shows the number of days each year when wave conditions (Hs) would meet the threshold criteria shown in Figure 33. The GAB site shows a strong persistent swell, with only 35 days per year with Hs below 2.5 m, no other site has fewer days with Hs below 2.5 m. The Brazilian site is the calmest in terms of Hs and most days have Hs below 2.5 m.

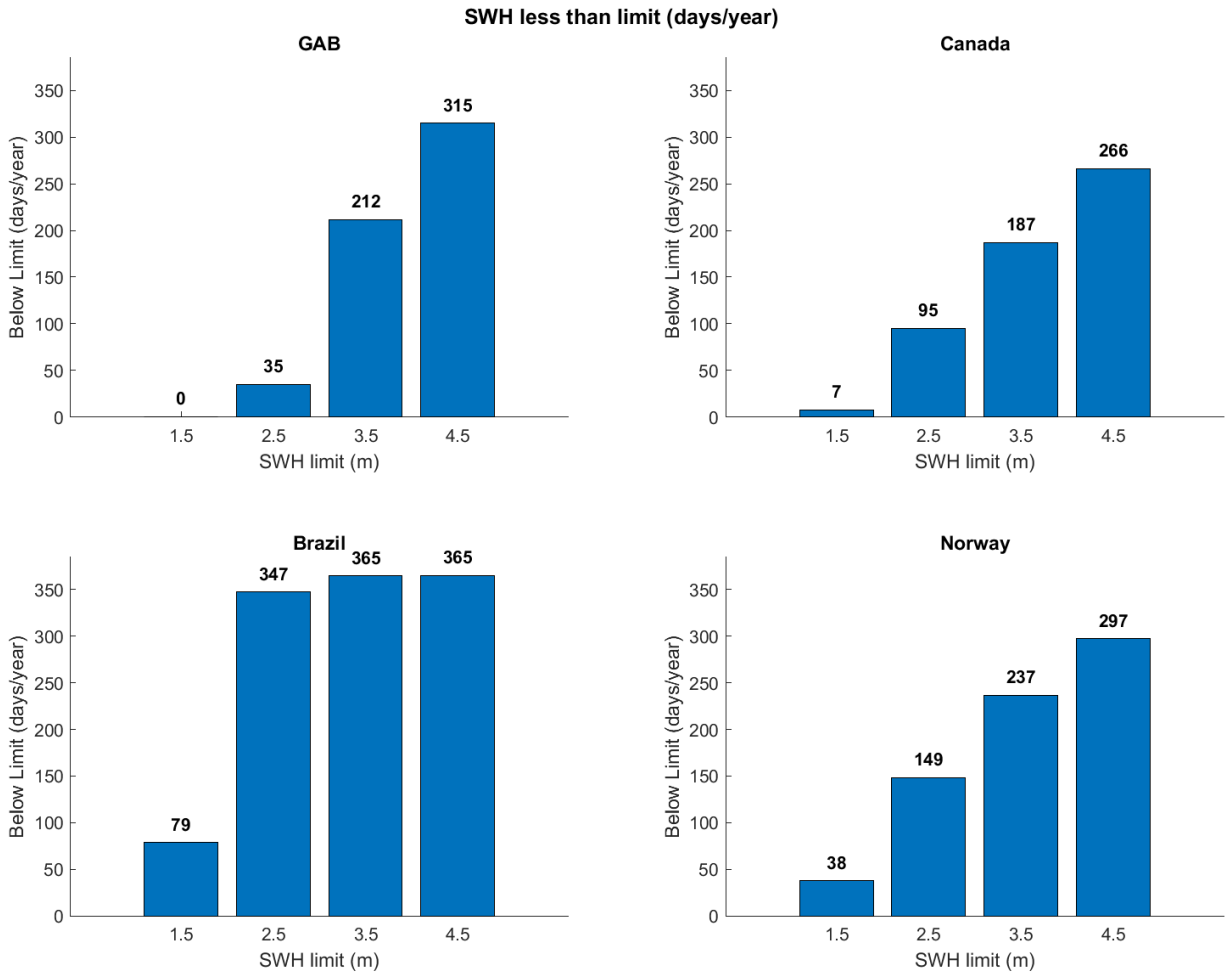

Figure 34. Estimated number of days a year with 5 consecutive days of significant wave height below the threshold limit.

Similar analysis of periods of five consecutive days or more below wind speeds ranging from gentle breeze (<10 knots) to gale force (>30 knots) for each location is shown in Figure 35. At the GAB site, during the 40-year period of the ERA-interim output, there were only a few events where wind speed was continuously below 10 knots for 5 days. For the 40 year period, this was still effectively 0.0% of the record length. There were relatively few periods (<15% of the time) where wind speeds were below 15 knots. At the Canadian and Norwegian sites wind speed was only below 15 knots for approximately 3.5% and 14% of the time, respectively.

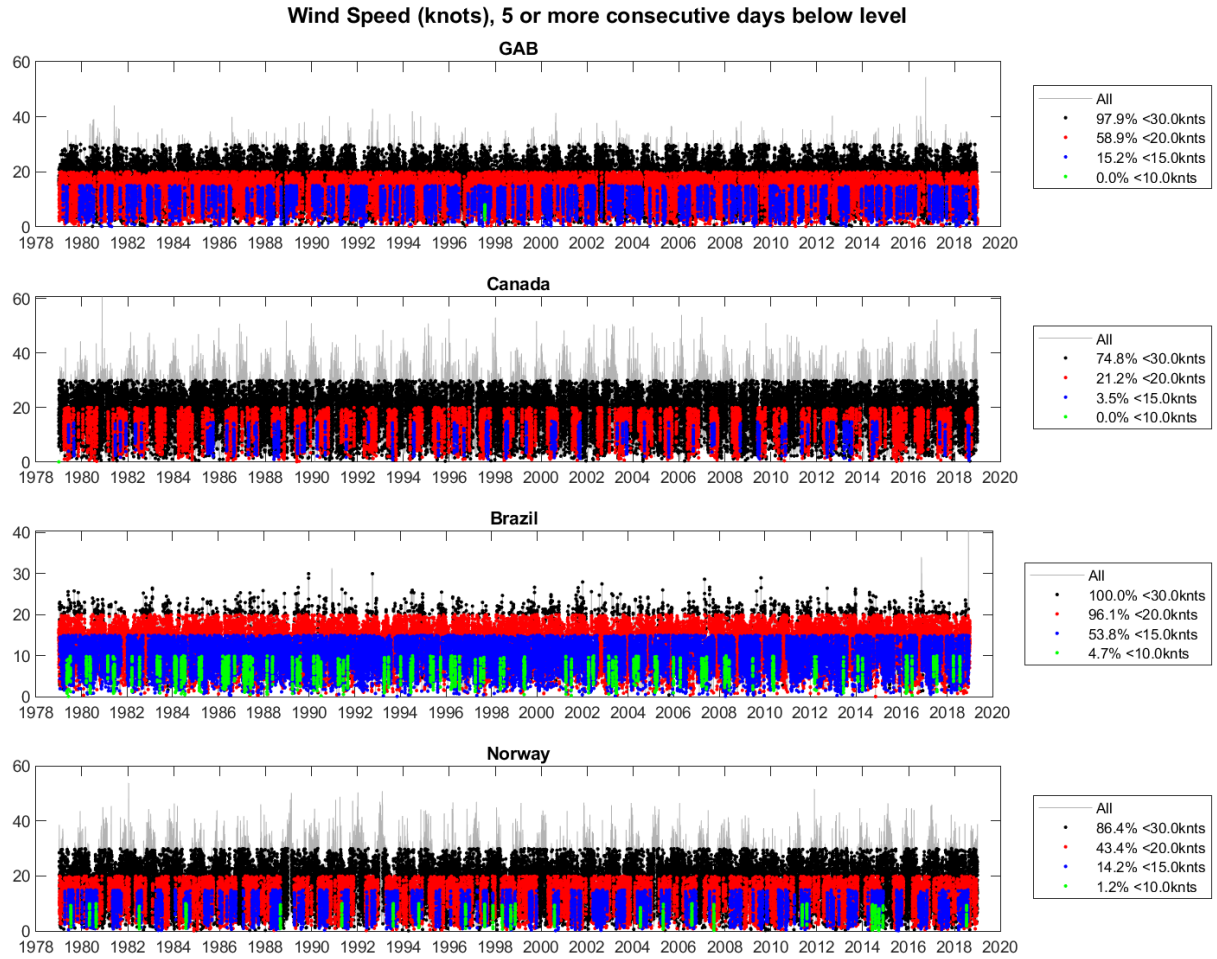

Figure 35. Full 40-year wind speed output for all four sites, highlighting, by colour, periods of 5 of more days below the specified wind speed thresholds. The percentage of time as a function of the entire record where these conditions were met are summarized next to each time series.

Figure 36 shows the number of days each year when wind speeds would meet the threshold criteria shown in Figure 35. The GAB site shows persistent winds above 15 knots with only 55 days per year below this threshold level. The Brazilian site is the calmest in terms of wind speed, followed by the GAB with Norway and Canada showing the strongest winds.

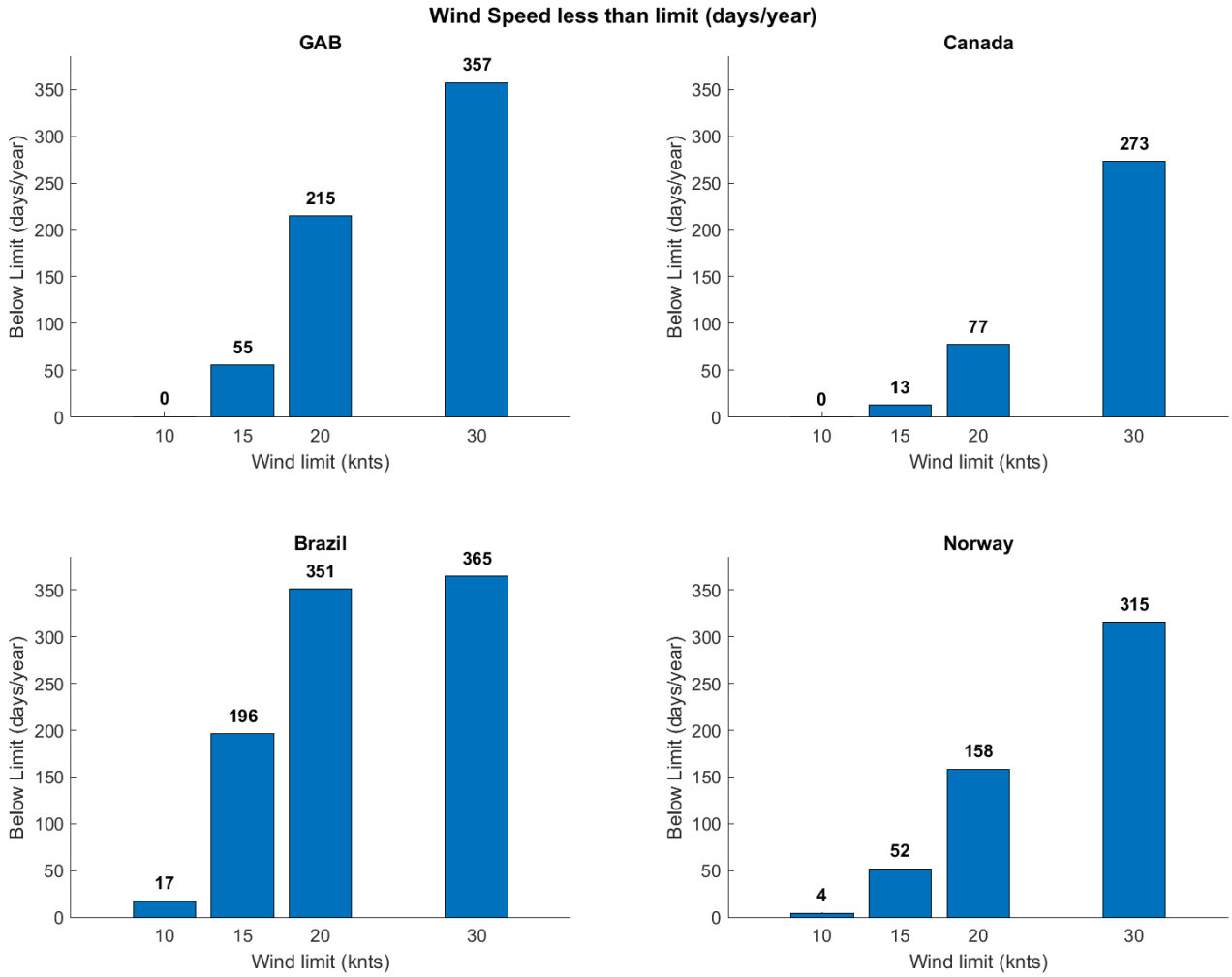

Figure 36. Estimated number of days a year with 5 consecutive days of wind speed below the threshold limits.

Discussion

There has been concern from commercial fisheries and the community regarding the suitability of the Great Australian Bight (GAB) offshore environment for hosting offshore petroleum activities given the exposed nature of the site. Due to the remoteness of the GAB, the long time-series of direct observations (e.g. wind, waves, and currents) necessary for developing a quantitative understanding of environmental variability, trends and extremes relevant to offshore petroleum activities are not available. To bridge this gap, long time-series generated from a suite of global data-assimilating and reanalysis models were analysed to characterise and compare the offshore conditions expected in the GAB with three other major international offshore deep water petroleum locations.

The comparison shows that the two North Atlantic sites, located in Canada and Norway, were exposed to the strongest winds and highest waves, followed closely by the GAB. All sites, except for Brazil, are expected to experience Gale force (>62 km/h) winds and large waves (>6 m) on a yearly basis. Winds at the GAB site were characterized by a pronounced seasonal signal and were typically stronger in summer and winter than during spring and autumn. Predominant wind directions were from the southeast in summer and southwest in winter. Wind speeds during these seasons regularly reached 60 km/h. Notably, periods of calm wind conditions were rare, with winds persistently greater than 15 knots year round.

The GAB site is located in a high energy wave environment and is exposed to a remarkably consistent surface wave field characterised by significant wave heights greater than 2.5 m from the southwest year round. Maximum wave heights of 17.4 m are expected for a one hundred year return period. Trend analysis indicated significant increases in monthly average significant wave height (Hs) are occurring during the summer (February) and winter (July). Trends in monthly averages could be caused by changes in the timing or number of storm events occurring in the Southern Ocean, which is the source of the dominant swell in the GAB. Global comparisons showed the peak wave period was largest in the GAB because the region receives swell waves generated by distant storm systems over a large fetch. Similar to winds, and relative to other locations, wave conditions in the GAB site were rarely calm, with significant wave heights less than 1.5 m for 5 consecutive days occurring only once over the 40-year model reanalysis.

Current speeds at the GAB site were comparable to other locations but showed the greatest directional variability, particularly when comparing the directional changes between surface and deep layers. Current directions in the GAB were most variable in the ocean surface layer (0-50 m), with maximum speeds of 30 cm/s directed towards the northeast to southeast. This

is equivalent to approximately 25 km/day. At mid-depths (50-200 m) current directions were less variable and predominantly to the southeast with maximum speeds of approximately 17-20 km/day. Deeper currents (200-4000 m) were directed on- and along-shore to north and east, with maximum speeds slightly less than that observed at mid-depths.

This report provides a detailed characterisation, assessment and prediction of the met-ocean conditions that will be encountered by, and have the potential to impact, future petroleum activities in the GAB. In the absence of direct, long-term observations, the improved understanding of the offshore GAB environment generated by this study is critical to the assessment of the suitability of the GAB for hosting offshore petroleum industry and response planning necessary to mitigate any environmental impacts that may result from associated activities. By providing comparisons to the environmental conditions experienced at several major international offshore petroleum locations, the information in this report provides the clarity and context needed by South Australian fishing and aquaculture sectors, and the broader community, to make informed decisions regarding met-ocean interactions with petroleum activities in the GAB.

Implications

Commercial fishing and aquaculture in the GAB generates approximately 25% of Australia's total seafood value, contributes over $400 million per year into the State economy and makes a significant socio-economic contribution to surrounding regional communities (Pascoe and Innes, 2017). Outcomes from this project provide stakeholders in the ASBTIA, and other commercial and recreational users of the GAB, with information needed to understand and assess the suitability of the physical environment for hosting petroleum activities in the GAB in a global context. Site comparisons presented in this study indicate that whilst the two offshore petroleum sites located in the North Atlantic (i.e. Canada and Norway) are likely to experience the most extreme wind and wave conditions (e.g. strongest winds and largest waves) at times throughout the year, the GAB site experiences remarkably persistent medium to large high energy swells and strong winds year round. These differences in site exposure between the GAB and other offshore petroleum locations are likely to present different challenges to petroleum activities, such as the ability to respond to incidents.

The outcomes and outputs of this project have also demonstrated how global data-assimilating, reanalysis models can be used to provide quantitative information necessary to inform decision making in regions where there is a paucity of observations. This approach

would assist Australian fishing and aquaculture sectors, and the broader community, in assessing the long-term environmental sustainability of future offshore developments, including petroleum activities, in data poor regions along Australia's coast.

Recommendations and Further Development

It is recommended that the results of this study be broadly distributed to the state commercial fishery and aquaculture sectors, Government of South Australia Department of Primary Industries and Regions, Australian Fisheries Management Authority (AFMA), international oceanographic modelling scientists and the general public to provide a greater understanding of the sea-state and exposure of the GAB relative to other international offshore petroleum sites. Findings from this report provide quantitative information which can be used by various industry sectors and mangers to support decision making regarding the potential influence of environmental conditions on petroleum activities and the ability to respond to incidents in the GAB.

Additionally, the need to use coarse resolution global models in this project to fill observational gaps in the GAB highlights the requirement for both sustained high-resolution ocean models for southern Australia and more observational data in the central GAB region. Current validated hydrodynamic models provided through the eSA-Marine system (https://www.pir.sa.gov.au/research/esa_marine) and SARDI Aquatic Sciences are underpinned by Integrated Marine Observing System (IMOS) oceanographic observations made at locations on the shelf adjacent to Spencer Gulf near Kangaroo Island and eastern Eyre Peninsula. Collection of oceanographic data, including waves, in the central and western GAB, maintained over the long term, would improve model and extreme event predictions for the GAB region.

The paucity of ocean data for the central and western GAB region gas been identified by the Southern Australian Integrated Marine Observing System (SAIMOS) node as a key spatial gap in the observing system.

Extension and Adoption

The principle investigator presented preliminary findings at the ASBTIA and FRDC Industry workshop in November 2019 and will present the final outcomes at the workshop in November 2020.

Project results have been used by ABSTIA to inform their correspondence with NOPSEMA regarding petroleum exploration in the GAB.

Project coverage

Posted on PIRSA and FRDC Facebook pages.

Project materials developed

It is anticipated that data will contribute to the preparation of a peer-reviewed publication summarizing the climatology and trends of the offshore South Australian wave environment.

Statistical methods and data used in this project have been adopted into model validation studies assessing the performance of ocean models developed by SARDI including the eSA-Marine (https://www.pir.sa.gov.au/research/esa_marine) South Australian Regional Ocean Model.

References

Amante, C. and B.W. Eakins, 2009. ETOPO1 1 arc-minute global relief model: procedures, data sources and analysis. NOAA Technical Memorandum NESDIS NGDC-24. National Geophysical Data Center, NOAA.

Bendat, J.S. and Piersol, A.G., 1986. Random data: measurement and analysis procedures.

Darbyshire, J., 1952. The generation of waves by wind. Proceedings of the Royal Society of London. Series A, Mathematical and Physical Sciences, Vol. 215, No. 1122, pp. 299-328.

Dean, R.G., 1990. Freak waves: A possible explanation. In A. Torum & O.T. Gudmestad (Eds.), Water Wave Kinematics (pp. 609-612), Kluwer.

Dee, D.P., Uppala, S.M., Simmons, A.J., Berrisford, P., Poli, P., Kobayashi, S., Andrae, U., Balmaseda, M.A., Balsamo, G., Bauer, D.P. and Bechtold, P., 2011. The ERA-Interim reanalysis: configuration and performance of the data assimilation system. Quarterly Journal of the Royal Meteorological Society, 137(656), pp.553-597.

Doubell, M.J., Spencer, D., van Ruth, P.D., Lemckert, C. and Middleton, J.F., 2018. Observations of vertical turbulent nitrate flux during summer in the Great Australian Bight. Deep Sea Research Part II: Topical Studies in Oceanography, 157, pp.27-35.

Durrant, T., Greenslade, D., Hemer, M., Trenham, C., 2014. A global wave hindcast focussed on the Central and South Pacific. CAWCR Technical Report 070

Gringorten, I. I., 1963. A plotting rule for extreme probability paper. Journal of Geophysical Research, Vol. 68, No. 3, pp. 813-814.

Goldsworthy, S.D., Mackay, A.I., Bilgmann, L.M., Moller, L.M., Parra, G.J., Gill, P., Bailleul, F., Shaughnessy P., Reinhold, S.-.L., Rogers, P.J., 2017. Status, distribution and abundance of iconic species and apex predators in the Great Australian Bight. Final Report GABRP Project 4.1. Great Australian Bight Research Program, GABRP Research Report Series Number 15, 227pp.

Kämpf, J., Doubell, M., Gri_n, D., Matthews, R.L., Ward, T.M., 2004. Evidence of a large seasonal coastal upwelling system along the southern shelf of Australia. Geophysical Research Letters 31, L09310.

Middleton, J.F. and Bye, J.A., 2007. A review of the shelf-slope circulation along Australia's southern shelves: Cape Leeuwin to Portland. Progress in Oceanography, 75(1), pp.1-41.

Middleton J.F., Griffin, D., Luick, J., Herzfeld, M., Hemer, M., James, C., and Oke, P. (2017). Theme 1: physical oceanography of the Great Australia Bight. theme report. Great Australian Bight Research Program, GABRP Research Report Series Number 31, 18pp

Laloyaux, P., de Boisseson, E., Balmaseda, M., Bidlot, J.R., Broennimann, S., Buizza, R., Dalhgren, P., Dee, D., Haimberger, L., Hersbach, H. and Kosaka, Y., 2018. CERA-20C: A coupled reanalysis of the Twentieth Century. Journal of Advances in Modeling Earth Systems, 10(5), pp.1172-1195.

Oke, P.R., P. Sakov, M.L. Cahill, J.R. Dunn, R. Fiedler, D.A. Griffin, J.V. Mansbridge, K.R. Ridgway, A. Schiller, 2012: Towards a dynamically balanced eddy-resolving ocean reanalysis: BRAN3, Ocean Modelling, 67, 52-70.

Pascoe, S. and Innes, J., 2017. Great Australian Bight fisheries: economic and social benchmark study. Final Report GABRP Project 6.3 – PART A. Great Australian Bight Research Program, GABRP Research Report Series Number 24 a, 41pp.

Rogers, P.J., Ward, T.M., van Ruth, P.D., Williams, A., Bruce, B.D., Connell, S.D., Currie, D.R., et al., 2013. Physical processes, biodiversity and ecology of the Great Australian Bight Region: A Literature Review. CSIRO, Australia.

Rogers, P.J., Huveneers, C., Page, B., Goldsworthy, S.D., Coyne, M., Lowther, A.D., Mitchell, J.G., et al., 2015. Living on the continental shelf edge: habitat use of juvenile shortfin makos, *Isurus oxyrinchus*, in the Great Australian Bight, southern Australia. Fisheries Oceanography 24, 205–218.

Stansell, P., 2005. Distributions of extreme wave, crest and trough heights measured in the North Sea. 18 Technical Memorandum No. 755 Notes on the maximum wave height distribution. Ocean Engineering 32, 1015-1036.

Sverdrup, H.U. and Munk, W.H., 1947. Wind, sea and swell: theory of relations for forecasting (No. 303). Hydrographic Office.

Toffoli, A., Bitner-Gregersen, E.M., Osborne, A.R., Serio, M., Monbaliu, J. and Onorato, M., 2011. Extreme waves in random crossing seas: laboratory experiments and numerical simulations. Geophysical Research Letters, 38(6).

van Ruth, P.D., Patten, N.L., Doubell, M.J., Chapman, P., Rodriguez, A.R. and Middleton, J.F., 2018. Seasonal- and event-scale variations in upwelling, enrichment and primary productivity in the eastern Great Australian Bight. Deep Sea Research Part II: Topical Studies in Oceanography, 157, pp.36-45.

Ward, T.M., McLeay, L.J., Dimmlich, W.F., Rogers, P.J., McClatchie, S.A.M., Matthews, R., Kämpf, J., Van Ruth, P.D., 2006. Pelagic ecology of a northern boundary current system: effects of upwelling on the production and distribution of sardine (*Sardinops sagax*), anchovy (*Engraulis australis*) and southern bluefin tuna (*Thunnus maccoyii*) in the Great Australian Bight. Fisheries Oceanography 15, 191–207.